



HEALTH RISK ASSESSMENT OF THE HOODED OYSTER, *SACCOSTREA*
CUCULLATA (BORN, 1778) FROM LIBONG ISLAND, THAILAND



KITIYA KONGTHONG

A Thesis Submitted to the Graduate School of Naresuan University
in Partial Fulfillment of the Requirements
for the Master of Science in Medical Sciences

2023

Copyright by Naresuan University

HEALTH RISK ASSESSMENT OF THE HOODED OYSTER, *SACCOSTREA*
CUCULLATA (BORN, 1778) FROM LIBONG ISLAND, THAILAND



A Thesis Submitted to the Graduate School of Naresuan University
in Partial Fulfillment of the Requirements
for the Master of Science in Medical Sciences
2023

Copyright by Naresuan University

Thesis entitled "Health risk assessment of the hooded oyster, *Saccostrea cucullata*
(Born, 1778) from Libong Island, Thailand"

By Kitiya Kongthong

has been approved by the Graduate School as partial fulfillment of the requirements
for the Master of Science in Medical Sciences of Naresuan University

Oral Defense Committee

..... Chair
(Associate Professor Wisanu Thongchai, Ph.D.)

..... Advisor
(Natthawut Charoenphon, Ph.D.)

..... Co Advisor
(Assistant Professor Ittipon Phoungpetchara, Ph.D.)

..... Co Advisor
(Assistant Professor Sinlapachai Senarat, Ph.D.)

..... Internal Examiner
(Professor Sutisa Thanoi, Ph.D.)

Approved

.....
(Associate Professor Krongkarn Chootip, Ph.D.)
Dean of the Graduate School

Title HEALTH RISK ASSESSMENT OF THE HOODED OYSTER, *SACCOSTREA CUCULLATA* (BORN, 1778) FROM LIBONG ISLAND, THAILAND

Author Kitiya Kongthong

Advisor Natthawut Charoenphon, Ph.D.

Co-Advisor Assistant Professor Ittipon Phoungpetchara, Ph.D.
Assistant Professor Sinlapachai Senarat, Ph.D.

Academic Paper M.S. Thesis in Medical Sciences, Naresuan University, 2023

Keywords Apoptosis, Histological analysis, Heavy metal analysis, Risk environment assessment, Hooded oyster *Saccostrea cucullata* (Born 1778), Morphometric analysis

ABSTRACT

Libong Island is an important seagrass bed in Thailand, which has been impacted by the environmental crisis. The environmental changes should have negatively affected the health status of aquatic animals in the area, but few studies are available on this topic. In this study, the health status of a sentinel species, the hooded oyster *Saccostrea cucullata*, was addressed using organ development of field-collected *S. cucullata* associated with their shell size distributions, the multi-organ histopathology and apoptotic analysis along with the measurement of heavy metal bioaccumulation. The water quality parameters were not significantly different between the sampling areas except for the water temperature ($p < 0.05$). *S. cucullata* from the Stone Bridge site had smaller shell lengths and higher condition factors than those from Dugong Tourism by Drones except for the size of the organ. Histologically, the highest mean length of gill lamellae (192.1 ± 3.92 at 2.1-3 cm). The thinnest of the mantle epithelium (73.78 ± 3.08 μm in 4.1-5 cm) of *S. cucullata* showed and statistically significant difference between the sampled locations (Specific F value=0.1783 and 0.8605, $p < 0.01$, $p < 0.0001$). The density of mucous-secreting cells (Msc) was more prominently distributed in the digestive gland than in other tissues. The 2.1-3 cm group or bigger had mature gonads with protandric characteristics, showing rapid sexual differentiation in the Stone Bridge site. Moreover, gills, digestive glands, gonads, and

mantles of *S. cucullata* were collected from different monitoring a reason this island including the Stone Bridge site and the Dugong Tourism by Drones site. The highest health assessment index HAI values were recorded in the gill, whereas the lowest values were observed in the digestive glands. Histopathological alterations and heavy metal bioaccumulation were found in samples from both sites, but most HAI values and the density of apoptotic cells were significantly higher in samples from the Dugong Tourism by Drones site than those from the Stone Bridge site $p < 0.0001$. The highest values of heavy metal concentrations were in the digestive gland: zinc 638.38 ± 3.96 mg/kg¹ dry weight, copper 190.52 ± 0.44 mg/kg¹ dry weight, lead 23.36 ± 0.45 mg/kg¹ dry weight, and cadmium 961 ± 0.18 mg/kg¹ dry weight. The hazard quotient HQ values were > 1 , representing the moderately harmful levels for human consumption. The current knowledge about the use of multi-organ histopathology with the heavy metal bioaccumulation of *S. cucullata* might be noted in its undisturbed health and suggested that this oyster can be used to monitor marine pollution in Thailand. Long-term monitoring assessment and the environmental protection of Libong Island should be focused on as a more accurate environmental risk assessment.

ACKNOWLEDGEMENTS

My most profound appreciation goes to Dr. Natthawut Charoenphon, and Assistant Professor Sinlapachai Senarat, my Ph.D. advisors and mentors, for their time, effort, and understanding in helping me succeed in my studies. Their vast wisdom and wealth of experience have inspired me throughout my studies. In addition, I would like to be especially thankful to Assistant Professor Ittipon Phoungpetchara for their technical assistance throughout my research.

I would like to thank the NC-Patho laboratory junior student from Naresuan University, Racho Khaochomnan and the Marine science junior student from the Faculty of Science and Fisheries Technology, Rajamangala University of Technology Srivijaya, Trang Campus for your kind support on laboratory processing and sampling collection.

However, this research was supported by a scholarship to support the studies undertaken by Honors Graduates in the Master's degree at the Faculty of Medical Sciences, Naresuan University, and The King Prajadhipok and Queen Rambhai Barni Memorial Foundation for the year 2022. The preparation of samples was completed in the Marine Natural Product Laboratory of the Faculty of Science and Fisheries Technology, Rajamangala University of Technology, Srivijaya Trang Campus. All further preparation and analysis processes were completed in the Department of Anatomy, Faculty of Medical Science, Naresuan University. The chemical analysis has been completed in the Chemistry Laboratory at the Science Center, Faculty of Science and Technology, Pibulsongkram Rajabhat University. The processes have been completed in the Department of Anatomy, Faculty of Medical Science, Naresuan University.

Finally, I appreciate and thank my family, friends, and everyone who has been there emotionally and intellectually as I've worked on my research.

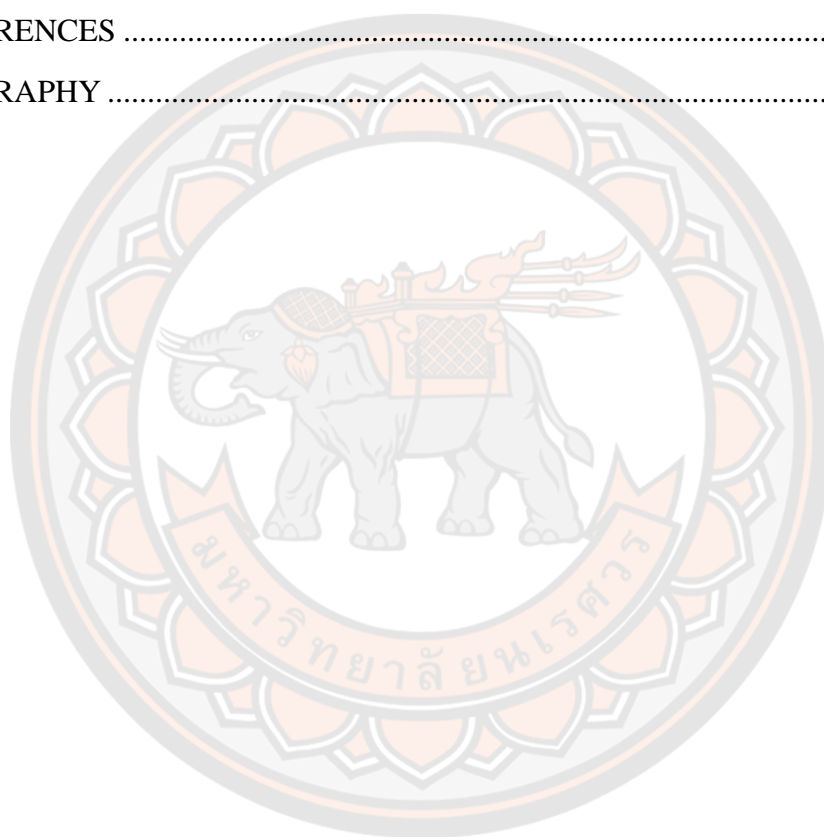
Kitiya Kongthong

TABLE OF CONTENTS

	Page
ABSTRACT.....	C
ACKNOWLEDGEMENTS.....	E
TABLE OF CONTENTS.....	F
LIST OF TABLES.....	I
LIST OF FIGURES.....	K
CHAPTER I INTRODUCTION.....	1
Background.....	1
Statement of the Problem.....	2
Objectives.....	2
Expected outcome.....	3
Scope of the Study.....	3
Key Words.....	3
CHAPTER II LITERATURE REVIEW.....	1
1. Marine bivalves as sentinel species and biology of the hooded oyster.....	1
1.1 Marine bivalves as sentinel species.....	1
1.2 The biology of hooded oysters.....	2
1.3 Integrated biomarkers.....	2
2. Libong island and its marine environmental problems.....	4
3. Heavy metal pollution.....	4
3.1 Toxicity of heavy metals on aquatic organisms.....	5
3.1.1 Cadmium (Cd).....	6
3.1.2 Lead (Pb).....	7
3.1.3 Copper (Cu).....	8
3.1.3 Zinc (Zn).....	9
3.2 Effects of heavy metal toxicity on aquatic organisms.....	10

4. Risk assessment	11
4.1 Risk Assessment.....	11
Risk Assessment.....	11
4.1.1 Hazard Identification	11
4.1.2 Hazard Characterization	11
4.1.3 Exposure Assessment	11
4.1.4 Risk Characterization	11
4.2 Risk Management.....	12
4.2.1 Risk evaluation	12
4.2.2 Development of risk management plan.....	12
4.2.3 Implementation of risk management plan	12
4.2.4 Monitoring and review	12
4.3 Risk Communication.....	12
CHAPTER III METHODOLOGY	13
1. Study areas and <i>Saccostrea cucullata</i> collection.....	13
2. Morphometry and morphological examination	14
3. Histological evaluations	15
4. In situ apoptosis detection using the TUNEL assay	22
5. Heavy metal analysis	23
6. Human Health Risk Assessment (HRA)	24
7. Statistical analysis	26
CHAPTER IV RESULTS.....	27
1. Water quality parameters	27
2. Shell size distribution in relation to histological development	28
3. Gonad development	33
4. Distribution of mucous-secreting cells	37
5. Histology and histopathological alteration of <i>S. cucullata</i>	39
5.1 The digestive gland	39
5.2 Gill lamellae	39

5.3 The mantle epithelium.....	39
5.4 The gonadal acini	41
6. Heavy metal accumulations in relation to the density of apoptotic cells	44
7. Human health risk assessment	46
CHAPTER V DISCUSSION AND CONCLUSION	47
Discussion.....	47
Conclusion	51
REFERENCES	52
BIOGRAPHY	67



LIST OF TABLES

	Page
Table 1 The tissue processing protocol for <i>S. cucullata</i> samples	20
Table 2 Histological characteristics of <i>S. cucullata</i> observed in this study	21
Table 3 AAS instrument parameters	24
Table 4 Input parameters to calculate CDI	25
Table 5 The oral reference dose (RfD) for the four heavy metals tested in this study	25
Table 6 HQ values and corresponding hazard risk levels	26
Table 7 The environmental factors between the sampling sites	27
Table 8 Morphometric measurement based on the different sizes of <i>S. cucullata</i> between Stone Bridge and Dugong Tourism by Drones site	29
Table 9 The condition factor (g/cm ³) of the sampled <i>S. cucullata</i> between Stone Bridge and Dugong Tourism by Drones site	30
Table 10 Type of male gonad of the <i>S. cucullata</i> from Stone Bridge and Dugong Tourism by Drones site	33
Table 11 The characteristics of spermatogenesis stage and oogenesis stage of the <i>S.</i> <i>cucullata</i>	35
Table 12 Oocyte development in four stages of <i>S. cucullata</i> between two sites study	36
Table 13 Percentage of sex difference of the <i>S. cucullata</i> between two locations	36
Table 14 Density of mucous-secreting cells in three tissue of the <i>S. cucullata</i> between Stone Bridge and Dugong Tourism by Drones site	38
Table 15 Mean range and standard deviation of heavy metal toxicity concentration (mg/kg ¹ dry weight) in the four tissue of <i>S. cucullata</i> from sampling locations	45

Table 16 The chronic daily intake and the hazard quotient of the heavy metals of the *S. cucullata* specimens between the Stone Bridge site and the Dugong Tourism by Drones site46



LIST OF FIGURES

	Page
Figure 1 Three main steps when responding to risk are: Risk Assessment, Risk Management, and Risk Communication (modified from Bekiari and Manoli, 2016).	12
Figure 2 The sampling sites at Libong Island, Thailand. (A-B) Overview of Libong Island. (C-E) The two <i>Saccostrea cucullata</i> 's collection areas on this island include the Stone Bridge site (Blue head arrow, D) and the Dugong Tourism by Drones site (Yellow head arrow, E).....	14
Figure 3 Morphometric measurement of the <i>S. cucullata</i> . Shell height (A), shell length (B), and shell width (C) all in millimeters (Cardoso et al., 2021)	15
Figure 4 Hooded oyster, <i>Saccostrea cucullata</i> . (A) Transverse sections were collected (between the lines) by performing two plans with a Low-Profile Disposable Microtome Blade. (B) Gross anatomy of <i>S. cucullata</i>	16
Figure 5 Schematic diagram for the entire experimental procedure. (A) Flowchart for the all steps of the protocol. (B) Schematic diagram illustrating the procedure for embedding large organs (take the macaque hemisphere as example, Kongthong et al., 2022).	17
Figure 6 Schematic diagram for the entire experimental procedure showed Hematoxylin & Eosin staining protocol for <i>S. cucullata</i> samples (Kongthong et al., 2022)	18
Figure 7 Masson's trichrome staining protocol for <i>S. cucullata</i> samples (Kongthong et al., 2022)	19
Figure 8 Digital image analysis process from ImageJ for the <i>S. cucullata</i>	22
Figure 9 Histological observations of different tissues of <i>S. cucullata</i> . (A) The cross-section of <i>S. cucullata</i> showed the position of the digestive gland, gills, and mantle epithelium tissue. (B) Digestive gland histology showed the primary and secondary ducts. (C) Gill filaments extended toward the side; the cilia were observed on their surface. (D) The mantle layer in the vesicle mass with the connective tissue. Abbreviations: Dg, Digestive gland; pd, primary ducts; sd, secondary ducts; G, Gills; c, cilia; M, Mantle; Go, Gonad.	31

Figure 10 Light microscope observation of the male gonad of *S. cucullata*. The spermatogenesis was observed in the visceral mass. (A) The mature gonad in gonadal acini (GA), (B) and spermatogonia (arrow). (C-D) The gonadal acini contained primary spermatocytes, secondary spermatocytes, Spermatids and spermatozoa. Abbreviations: Sg, Spermatogonia; Psc, Primary spermatocytes; Ssc, Secondary spermatocytes; St, Spermatids; Sz, Spermatozoa.32

Figure 11 Light microscope showed the female gonad development of the *S. cucullata* in follicle. (A) Oocytes in prematuration stage with immature oocytes that stored connective tissue. (B) Mature oocytes can be found in the follicles. (C-D) The mature stage contained many mature oocytes and absent the interstitial tissue. (E-F) Mature oocytes in the spent stage and surrounded by follicular cells. Abbreviations: SCT, Storage Connective Tissue; FC, Follicular Cells; O, oogonium; M, mature oocyte; CNT, Connective Tissue.34

Figure 12 The light microscope of mucous-secreting cells of the *S. cucullata*. Masson's trichrome staining. (A) Cross section of *S. cucullata* presented mucous-secreting cells in four types. (B) Mucous cells in gill filament with cup-like and stick-like shapes (arrow). (C) The secondary digestive tubules show mucous cells of oval and cup shapes (arrow). (D) Mantle epithelium cells show large mucous cells. Abbreviations: O, Oval or circle-like; C, cup-like; S, Stick-like; P, Pear-like.37

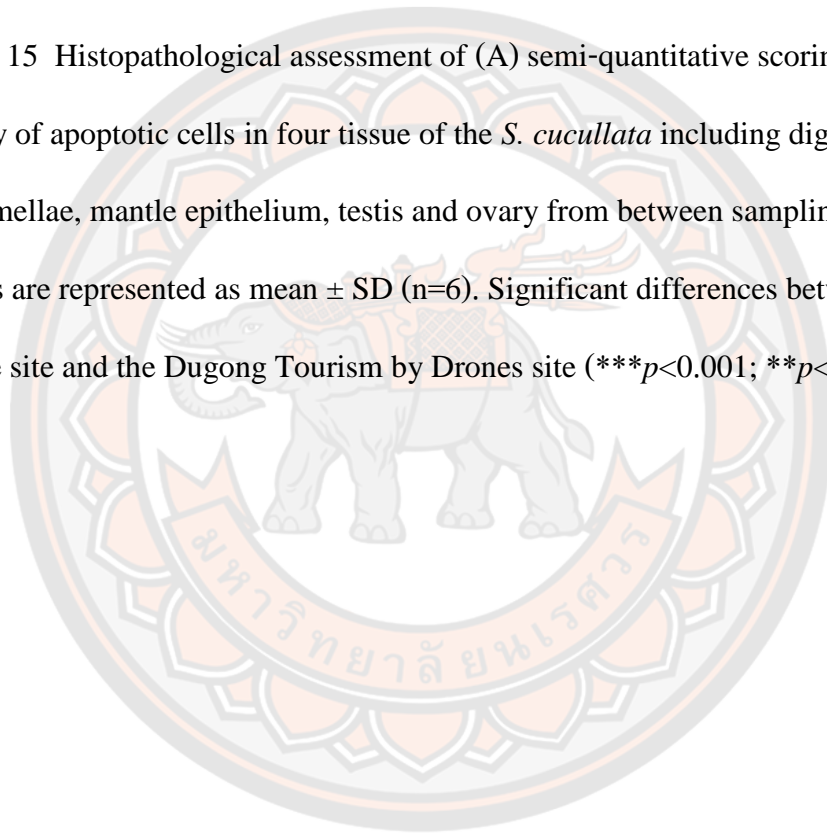
Figure 13 Histopathological alteration and the presence of apoptotic cell in the of the *S. cucullata* tissue between the Stone Bridge and the Dugong Tourism by Drones site.

(A-B) Digestive tubules regression with the appearance of apoptotic cell in the digestive epithelium (head arrows). (C-D) Gill lamellae fusion and hemocytic infiltration as well as the presence of apoptotic cell (head arrows). (E-F) Lipid vacuoles and mucocytes in the mantle epithelium throughout the visible of apoptotic cell (head arrows). (G) TUNEL-positive control. Abbreviations: Dt = Digestive tubule, tr = tubules regression; pd = primary ducts; sd = secondary ducts, L = Lumen, G = Gill lamellae, lf = lamellae fusion, M = Mantle epithelium, mc = mucous cells, lv = lipid vacuole.40

Figure 14 A photomicrograph of reproductive organ of the *S. cucullata* collected from the Stone Bridge and Dugong Tourism by Drones. (A) The histopathological lesion of the testicular showed the syncytium of spermatozoa and (B) TUNEL-positive were also observed at high magnification (100x, arrow). (C) Ovarian contained the oocytes with the vacuolar degeneration (Vd) at higher magnification and (D) black arrowheads was signifying the dark brown expression of TUNEL-positive cells. Abbreviations: Tt = Testis, syt = syncytium of spermatozoa, Oo =

Oocytes, FC = Follicle Cells, vd = vacuolar degeneration41

Figure 15 Histopathological assessment of (A) semi-quantitative scoring and (B) The density of apoptotic cells in four tissue of the *S. cucullata* including digestive gland, gill lamellae, mantle epithelium, testis and ovary from between sampling locations. Values are represented as mean \pm SD (n=6). Significant differences between the Stone Bridge site and the Dugong Tourism by Drones site ($***p<0.001$; $**p<0.01$).....43



CHAPTER I

INTRODUCTION

Background

Animal-based sentinel systems have been used to assess the impact of environmental problems, warranting the need for environmental monitoring in many locations (National Research Council, 1991; Aguirre-Rubí et al., 2018). The sentinel species should meet several conditions: its biology is well-known; the species is abundant in the environment and can be captured easily and its taxonomic features are characteristic and easily identifiable (National Research Council, 1991). Oysters commonly fulfill these requirements and have been widely used as a sentinel species in environmental and ecotoxicological studies (Lu-Yan et al., 2021; Pakingking et al., 2022; Jahan and Strezov, 2019). Jahan and Strezov (2019) used the Sydney rock oyster *Saccostrea glomerata* as a sentinel species due to its sessile and filter-feeding nature and abundance to assess the effect of trace elements in Australia. Luo et al. (2014) also used the Hong Kong oyster *Crassostrea hongkongensis*, reporting the zinc bioaccumulation. Indeed, bivalves including *Ruditapes philippinarum*, *Paphia undulata*, and *Crassostrea iredalei* (Lu-Yan et al., 2021; Pakingking et al., 2022) are generally good sentinel species that accumulate environmental contaminants more efficiently than crustaceans and fishes (Rodney et al., 2007; Pham, 2020). The use of oysters, however, could have an extra benefit since oysters are directly used for human consumption, and the accumulation of environmental contaminants may cause a serious health hazard (Sithole et al., 2022; Wang et al., 2022; Fang et al., 2001).

Histopathology is a popular tool for environmental assessment used in many biomonitoring programs of heavy metal pollution (Lushchak, 2011; Chandurvelan et al., 2013; Nguyen et al., 2018). It is also used for laboratory investigations, showing that heavy metal toxicity causes cell damage and dysfunction in aquatic organisms (Lushchak, 2011; Chandurvelan et al., 2013). In bivalves, haemocytic infiltration, lamellar fusion, and necrosis of gill are typical histopathological alterations as reported in *Anodonta cygnea* (Khan et al., 2018) and *Ostrea edulis* (Da Silva et al., 2006).

Chandurvelan et al. (2013) also reported increased hyalinocytes and apoptotic cells in gills of green-lipped mussel *Perna canaliculus* experimentally exposed to cadmium (Cd), suggesting immune responses and genotoxic damages.

The hooded oyster *Saccostrea cucullata* (Born, 1778), belonging to the family Ostreidae (Ramadhaniaty et al., 2018), is an economically important bivalve and a popular seafood, which is ubiquitously and abundantly distributed along the coast of Libong Island, Thailand (Pradit et al., 2020; Stankovic et al., 2021). This area is highly impacted by various environmental problems such as the occurrence of microplastics (Pradit et al., 2020) and heavy metals (Kobkeatthawin et al., 2021) because of the increased human and agricultural activities. These situations should also have impacted aquatic animals in the Libong Island area, but the assessment of aquatic animal health from this area is limited. In this study, we used *S. cucullata* as a sentinel species to monitor the environmental health in the Libong Island with a special focus on heavy metals. The integrated biomarkers include the multi-organ histopathology, apoptotic analysis, and heavy metal bioaccumulation. The health assessment index (HAI) and Human Health Risk Assessment (HHRA) index were calculated to quantitatively analyze the results. This report would provide valuable baseline data for the continuous monitoring for the environmental status of Libong Island and would also be important to assess the risk of humans who consume the oyster.

Statement of the Problem

The hooded oyster, *Saccostrea cucullata* from the coast of Libong Island that has been affected by human activities was unhealthy. High levels of heavy metal contaminations were also found in the selective tissue of oysters, indicating that they are unsafe for human consumption.

Objectives

The purpose of the study is to monitoring the health status of aquatic animals living in contaminated habitats can be a vital tool for assessing the level of exposure to heavy metals. Within the two objectives as following:

1. To investigate the morphological characteristics, structure, histopathological alteration and analysis of apoptosis in the soft tissue of the hooded oyster, *Saccostrea cucullata* from Libong Island, Thailand.
2. To evaluate the concentrations of four toxic heavy metals (Lead, Cadmium, Zinc and Copper) in the soft tissue of the hooded oyster, *Saccostrea cucullata* from Libong Island, Thailand.

Expected outcome

This study has the expected outcome as follows:

1. Get the safety of oyster consumption
2. Get the contaminate level of heavy metal toxicity in oyster

Scope of the Study

The hooded oysters, *Saccostrea cucullata*, were field collected in April 2022 at two locations in Libong Island, Thailand, including Stone Bridge. At locations close to the sand beach there was minor life-threatening human activity. The Dugong Tourism by Drones site there was major life-threatening tourist activity and near the seagrass beds. The physical and chemical parameters of water were also recorded. Integrated data were investigated with various biomarkers including morphological characteristics, histopathological lesions, and apoptotic cells throughout the heavy metal accumulation in selective tissues. Analysis of the integrated biomarkers was used to evaluate the health risks of oyster consumption and assess safety for consumers

Key Words

Apoptosis, Histological analysis, Heavy metal analysis, Risk environment assessment, Hooded oyster, *Saccostrea cucullata* (Born, 1778)

CHAPTER II

LITERATURE REVIEW

1. Marine bivalves as sentinel species and biology of the hooded oyster

1.1 Marine bivalves as sentinel species

Use of sentinel species is currently a common method to assess environmental contamination. Ideally the animal sentinel species used should be abundant, easy to sample, and respond rapidly to exposure to toxins in contaminated environments by accumulating the toxic substance in their tissue or organs. (National Research Council, 1991; Aguirre-Rubí et al., 2018; Amadi et al., 2020). Marine bivalves are well suited for use as sentinel species. They are filter-feeders consuming microalgae and suspended organic matter through filtration of water. The large filtration capacity of marine bivalves allows them to efficiently accumulate and concentrate within their soft tissues a variety of substances dissolved in the water (Lu et al., 2017; Baralla et al., 2021). Vaezzadeh et al. (2017) reported that mangrove oysters, *Crassostrea belcheri*, were collected from mangrove forests on the west coast of the Malaysian Peninsula, near areas of industrialization and urbanization. They investigated polycyclic aromatic hydrocarbons (PAHs) in the soft tissue of this species. The results showed concentrations of PAHs ranging from 309 to 2225 ng g⁻¹ (DW) in the mangrove oysters. This high concentration of PAHs accumulated in the oysters affected other species connected via food webs. Swaleh et al. (2016) investigated the bioaccumulation of heavy metals in two mollusk species (*Saccostrea chocolate* and *Mytilus edulis*) which were collected from Tudor Creek in Mombasa, Kenya in areas affected by human activities such as fisheries, tourism, and urbanization. The results indicated that *Saccostrea cucullata* accumulated higher levels of cadmium and lead than did *Mytilus edulis*, and that the amount represented a health risk to humans if consumed.

1.2 The biology of hooded oysters

The hooded oysters, *Saccostrea cucullata* are a filter feeder in the aquatic invertebrate group. They push water through their gills in order to feed on microalgae and phytoplankton. These oysters live on a solid surface such as mangrove roots, rocks, or manmade structures. Their habitat is the intertidal zone (Vaezzadeh et al., 2017)

Taxonomic classification (World Register of Marine Species / WORMS, 2018)

Order Ostreoida

Family Ostreaeidae

Genus *Saccostrea*

Species *Saccostrea cucullata* (Born, 1778)

The shell morphology and hinge structure are used for classification. It is reported that there are three main species of economic importance for fisheries in Thailand: *Saccostrea cucullata* (Born, 1778), *Crassostrea belcheri* (Sowerby, 1871) and *Crassostrea iredalei* (Faustino, 1932).

Hooded oyster reefs are usually found in coastal areas. The oysters' shells are composed mostly of calcium carbonate. There are two unsymmetrical halves of the shell, which are referred to as the "valves" of the oyster. These valves (half shells) are connected to one another at a hinge with a pair of adductor muscles, which control the opening and closing of the valves. Within the hooded oyster, the mantle secretes the valves. The ctenidia, commonly called the gills, are respiratory organs that siphon, filter, and move suspended organic matter into the stomach. There is also a circulatory system, albeit a simple one (Santhanam, 2018). Hooded oysters are hermaphrodite, with most young individuals beginning life as male. Later on the sex ratio becomes approximately equal as some become female, and in the end most individuals are female.

1.3 Integrated biomarkers

Biomarkers in analytical chemistry and environmental science are recognized as chemicals, metabolites, or changes in the body associated with an organism's exposure to a chemical. Biomarkers have the potential to determine whether exposure has occurred, the direction of exposure, the route of exposure, and the consequence of the exposure. (Wikipedia, "Biomarkers of exposure assessment"). In

general, there are three types of biomarkers. One is biomarkers of exposure. These are indicators of chemical exposure, in which biochemical and physiological changes are observed in tissues exposed to toxins in contaminated environments. Thus biomarkers of exposure are often used to assess the effects of toxic chemicals that may be harmful to health. The second type is biomarkers of effect, which are indicators of organ dysfunction after exposure to a toxic. Finally, there are biomarkers of susceptibility, which are indicators of susceptibility in response to toxic exposure (Lionetto et al., 2019).

In order to assess the health of the sentinel species, a bio-monitoring program must be designed to study the effects of exposure on specimens living in contaminated habitats. Histopathological alterations are a convenient method /biomarker of effect which, through relatively simple procedures, can show the presence of lesions in the target organs (Howard et al., 2004). For example, Hong et al. (2017) conducted a marine environmental quality assessment near industrial areas in Southern Malaysia state and East Malaysia. In that study, tropical oysters (*Crassostrea iredalei*) were first examined for macroscopic symptoms and then processed for histological analysis. The histopathology alterations including hypertrophy, hyperplasia, and necrosis were found. Similarly, Os (2017) researched biomarker responses of *Crassostrea virginica* to trace metals and water-quality parameters, especially in terms of environmental stress, using histopathological observation including gills, guts, gonads and interstitial tissues of the mollusk. Histopathological lesions showed that those oysters are sensitive to environmental changes, which result in atrophy of digestive diverticula and gill tissue.

Apoptosis is programmed cell death via extrinsic and intrinsic pathways that can cause by infectious or effect of exposure to a contaminated environment, which induced cell injury and cell death. Apoptotic cells were found both of aquatic vertebrates and invertebrate including cnidarian, sea urchins and marine bivalves etc. (Lasi et al., 2009; Galasso et al., 2019; Yavasoglu et al., 2016). Sunila and Banca (2003) presented apoptotic cells in the oysters, *Crassostrea virginica* around Long Island Sound in The United State. The oysters were infectious of *Perkinsus marinus* into connective tissue such as gill, stomach and epithelium cells. The histopathological lesion found the hemocytes. As well as the result of Yavasoglu et al. (2016) were

observed histological alterations in the hepatopancrease and gills including degeneration in the digestive tubules, cellular swelling in the epithelial cells from the Izmir coast at Turkey.

2. Libong island and its marine environmental problems

Libong Island is located in southern Thailand, where there are extensive seagrass beds (more than 12,000 square meters). However, seagrass ecosystems are currently being lost at the rate of 3.2% per year (Stankovic et al., 2021). Seagrass ecosystems are endangered from various factors, both environmental factors and anthropogenic activities such as trawl fishing, sedimentation, marine tourism, construction at Kantang Port, coastal development with land reclamation, agricultural wastewater runoff, industrialization, and urbanization. According to the Department of Industrial Works (2021), Kantang District has a total of 49 industrial factories that manufacture items such as food products, wood products, rubber products, auto parts, and industrial manufacturing equipment. The wastewater discharged by many factories into the Trang River does not meet established safety standards. A total of more than 2,570 cubic meters of treated wastewater are discharged every day, and these effluents are often contaminated with toxic material, heavy metals, and organic material are loaded into the river and accumulate in the sediment before being carried by tides out into the sea. This causes environmental changes for aquatic organisms. However, there have been no previous studies collecting integrated data assessing bivalve health in the area.

3. Heavy metal pollution

Rapid industrialization, agriculture, and urbanization have caused increasing pollution such as wastewater, garbage, and pesticide residues, all of which directly affect the aquatic environment, especially at estuaries where there is a confluence of rivers before they flow into the sea. Sediment and garbage often carry heavy metals and other contaminants to an area. This can be seen in the results of an impact study on dredging the seabed for Gladstone Harbour, a port near the Great Barrier Reef in Australia. Dredging can also cause the direct death of seagrass beds and contamination of aquatic organisms with copper, arsenic, zinc, PAHs, and TBT (Dennis et al., 2016).

Katang Port is located at estuaries, and it is a busy center of boat construction, including the painting of boats. Antifouling paint is used to coat boat hulls to protect them from barnacles, and this practice is highly toxic to the aquatic environment (Bryan et al., 1986). Particularly for marine bivalves, the high toxicity of antifouling paint can cause abnormal valve morphology and also affect female growth in some species, resulting in a decrease of the marine bivalve population (Landos et al., 2021).

Hooded oysters, *Saccostrea cucullata* are a popular seafood for tourists and a commercially important export, but they usually have heavy metal contamination from their habitat. Heavy metals are generally considered those with a specific density higher than 5 g cm^{-3} , which makes them slow to decompose and enables them to accumulate in the environment for a long time. Heavy metals vary in the intensity of their toxicity to consumers. In particular, mercury, lead, cadmium, and copper are classified as heavy metals with high toxicity to human health, damaging the nervous system, liver, kidneys, and immune system, for example. Although in Thailand contamination of seafood by heavy metals and toxins is not supposed to exceed the standards set out by Public Health Ministry Order No. 414 in 2020, seafood is usually found to exceed those standards. In response to such contamination issues, Wang et al. (2018) developed a method for environmental monitoring of coastal pollution in China. They used the Hong Kong oyster, *Crassostrea hongkongensis*, as a biomarker to assess coastal pollution, and the results of that study as well as another showed that heavy metals such as lead, cadmium and copper exceeded the standards set by China's National Food Safety Standard for Healthy Foods (Lu et al., 2017). Thus, monitoring the health status of aquatic animals living in contaminated habitats can be a vital tool for assessing the level of exposure to heavy metals. Data collected in this way can help improve and ensure the safety of oysters consumed.

3.1 Toxicity of heavy metals on aquatic organisms

Heavy metals are environmental pollutants caused by human activities. Common heavy metals found in aquatic environment were copper, zinc, lead, and cadmium. Its can cause chronic and acute toxic poisoning and are usually found contaminated in oysters. Therefore, many consumers believe that these metal elements in oysters are harmful to human health. Metal elements are usually present in the aquatic

environment. Oysters absorb heavy metals from food and water flowing through their gills. Heavy metal uptake is often food-chain dependent and can be increased by bioaccumulation and subsequent biomagnification. These heavy metals and their effects on humans and the environment are summarized below.

3.1.1 Cadmium (Cd)

Cadmium is a nonessential metal with no biological function in aquatic animals (Rodney et al., 2007). Aside from chronic exposure, cadmium can affect marine organisms' growth, reproduction, immune system, and development, and behavior (Pham, 2020). In the environment, cadmium forms free cadmium ions (Cd^{2+}). These cadmium forms are the predominant mode of toxic responses in aquatic organisms. Water quality contributes to the transformation of cadmium to a state that is toxic to aquatic animals, such as pH, dissolved organic matter, and salinity. In marine environments, dissolved cadmium is predominantly a chloride complex associated with salinity. The toxicity of cadmium to aquatic organisms increases with decreasing salinity (Sun et al., 2018). This data can be found in estuary conditions. For example, in an oyster's habitat in an estuary, the eastern oyster *Crassostrea virginica* was exposed to cadmium in different concentrations in seawater for 96 h. The gills and digestive glands of the oyster were also determined when exposed to Cd (Adeyemi and Deaton, 2012).

Cadmium-contaminated water and food are absorbed in the stomach when ingested. The biological cadmium uptake pathways are the gastrointestinal and respiratory tracts. It has serious consequences in the blood by binding to high molecular weight proteins. It is also reported to cause various changes in the ecology of organisms because it accumulates mainly in the liver and has a half-life of 30 years (He et al., 2023). Due to cadmium poisoning, chronic exposure to Cd may cause kidney disease called "Itai-itai" (Nishijo et al., 2017). According to the United Nations Food and Agriculture Organization (FAO), the permitted level of cadmium in oysters is 0.2 mg/kg, which is the upper limit of consumption. Moreover, physical symptoms such as headaches, colds, sore throats, and sore hands may appear after eating cadmium-contaminated food. Long-term exposure to cadmium can lead to kidney disease and weak bones (He et al., 2023).

3.1.2 Lead (Pb)

Lead distribution in the sea depends on its chemical form; water quality such as acidity or alkalinity (pH), salinity, oxidation state, flow rate, suspended solids, and minerals; and organics. In particular, pH is of paramount importance in modulating the chemical properties of lead, such as solubility, precipitation, or organic complexation. In the environment, lead is contaminated in the river and deposited into the sediment, where its availability has adverse effects on aquatic organisms (Wang et al., 2022). The bottom sediment, as a sink in rivers or seas, can stay for longer periods and has limited mobility. Once absorbed in sediment, the lead compound reacts with other chemical species and transforms into a water-insoluble form (Fukunaga et al., 2011). Lead has a short half-life, adsorption, desorption, precipitation, and dissolution. The level of concentration can be decreased in the sea.

Among marine invertebrates, oysters are powerful filter feeders that absorb substances from water and food faster than losing these substances through metabolism and excretion. For example, in the marine bivalve species, *Crassostrea rhizophorae*, there is a detoxification mechanism that reduces lead toxicity by collecting lead in granules in the digestive glands (Wanick et al., 2012). Similarly, Fukunaga and Anderson (2011) reported that they found lead in low concentration in *Macomona liliana* due to its strong binding affinity to sediments and suspended particulate matter. However, we cannot exclude the possibility of high excretion rates by these oysters, resulting in low bioaccumulation. For this reason, these affinities may reduce organisms' absorption rate of this metal.

Bivalves can accumulate large amounts of heavy metals, especially lead, and their meat consumption can pose potential risks. Acute toxicity from ingestion of contaminated food is rare, but chronic exposure may have undesirable toxic effects. Lead is absorbed into the body and circulates through the circulatory system. It binds with red blood cells instead of iron (Fe^{+2}), an essential metal for red blood cell formation, causing anemia. According to the Food and Agriculture Organization of the United Nations (FAO), oysters' maximum permissible lead concentration is 0.3 mg/kg. Also, the U.S. Environmental Protection Agency has proposed that in 2021, 40 ug/dl of lead per day is the upper limit for adults and 10 ug/dl of lead per day for children.

3.1.3 Copper (Cu)

In coastal environments, natural concentrations of copper (Cu^{2+}) are low, but they are increasing due to human industrialization. At high concentrations, copper becomes toxic, affecting the metabolic processes of marine organisms. The toxic free-ion concentration of copper (Cu^{2+}) is predicted to increase by 115% in coastal waters in the next 100 years due to reduced pH (Pascal et al., 2010). Increased anthropogenic activities such as urbanization, industrialization, and agriculture can cause wastewater discharge into rivers containing a toxic form of copper called copper (II) sulfate (Cu_2SO_4). The increase in copper concentrations, which involves water quality, happens if the pH decreases and temperature increases in the aquatic system (Mesquita et al., 2019). The copper toxicity mechanism can explain these processes. In toxic form, it can act to begin the redox cycle. Hydrogen peroxide is converted into a hydroxyl free radical via a catalytic process and produces highly unstable reactive oxygen species (ROS), such as O^- and HO^- . For this state of copper toxicity, the metal can interact with functional groups, including carboxyl, hydroxyl, and sulfhydryl. Several studies have shown that increased ROS production can affect many metabolic pathways, such as glycolysis, protein, fatty acid, and amino acid metabolism. Moreover, cadmium toxicity does not only increase cellular ROS levels but also causes changes in lipid peroxidation and glutathione (GSH) levels in various cell types, suggesting that Cu-induced apoptosis may be associated with oxidative stress. (Galaris & Evangelou, 2002; Ferreira-Cravo et al., 2009; Chiarelli & Roccheri, 2014). In toxic form, copper (II) sulfate is very harmful to marine invertebrates such as crustaceans, cephalopods, and bivalves. In some species of bivalves or some of their life stages, this metal is found in the hemocyanin protein used for respiration, so the high concentrations of Cu detected should be considered with caution (Ferreira-Cravo et al., 2009; Mesquita et al., 2019). Moreover, high levels of copper are toxic to aquatic animals and may lead to cellular damage, such as histopathological changes in exposed oyster gonads and digestive glands (Osuna-Martínez et al., 2011).

Cu is often contaminated in oysters. In 2000, the Food and Agriculture Organization/World Health Organization recommended limiting Cu levels in oysters to 0.05 mg/kg. Also, ingestion of more than 1 g of copper sulfate could result

in chronic or long-term exposure to high levels of toxicity. Clinical symptoms of this condition include diarrhea, headache, and in severe cases, could induce renal failure.

3.1.3 Zinc (Zn)

Zinc is widely distributed in the environment and is an essential trace element for aquatic organisms and humans (Li et al., 2018). In nature, free Zn^{2+} ions are the predominant inorganic Zn species in most natural waters. Zn is already the most abundant trace metal in most marine environments, with natural concentrations in coastal waters ranging from about 0.1 to 20 micrograms per liter (Osuna-Martínez et al., 2011). It's often found in high concentrations in sediments (Li et al., 2018). It is strongly bound to organic compounds in the blood of benthic animals, with a half-life of about 21 days. (Wang et al, 2022).

Oysters are a high source of Zn. The Zn concentrations in oysters can reach 1-5% of dry tissue weights. The higher accumulated zinc contents without apparent toxicity indicate that oysters may have evolved a unique and mechanism intriguing zinc metabolic (Kong et al., 2020). Oysters absorb zinc from the water column through their gills and body surface, as well as by ingesting particulate matter. Also, oysters have the ability to regulate tissue zinc concentrations at very high levels. From previous studies, the Hong Kong oyster, *Crassostrea hongkongensis*, was obtained from sites contaminated in China, they found the oysters accumulated with different concentrations of heavy metals including zinc, copper, manganese, and lead. This investigation indicated that oysters respond to long-term heavy metal contamination. It has a high concentration of approximately 3.0% of Zinc (Luo et al., 2014). Moreover, Hietanen, Sunila, & Kristoffersson (1988) reported that the lethal concentration (LC_{50}) of 20.8 mg Zn/l showed an acute inflammatory response in the gills with dilated branchial veins, and the post lateral cells were swollen.

According to the National Institutes of Health, 40 mg of zinc per day is the upper limit for adults. Zn toxicity is a medical condition involving an overdose or toxic overexposure to Zn. Such levels of toxicity have been observed with Zn ingestions above 50 mg. Clinical symptoms of adverse effects from high Zn intake include nausea, vomiting, anorexia, abdominal cramps, diarrhea, and headache. These

clinical symptoms are associated with chronic effects such as weakened immune function (NRC, 1991).

3.2 Effects of heavy metal toxicity on aquatic organisms

Marine pollution with heavy metals becomes a severe situation for the aquatic environment and the organisms when concentrations of heavy metals exceed safe limits (Chiarelli and Roccheri, 2014). This impact caused by various anthropogenic activities released into rivers and seas has induced poor water quality. This is the leading cause of the increased hardness of heavy metals in the aquatic environment. Heavy metals are stable compounds, non-biodegradable, tend to accumulate in sediments, and have long half-life periods in the environment, making them hard to manage. Benthic animals take up heavy metals in sediments in a process called bioaccumulation. In the aquatic environment, phytoplankton is the primary product ingested by zooplankton, and then larger animals feed on these contaminated organisms, absorbing toxins into their bodies and increasing their concentrations in a process known as biomagnification. The metals can cause severe toxicity in aquatic animals by producing reactive oxygen species through oxidizing radical production and inducing the development of oxidative stress is the underlying molecular mechanism of metal toxicity (Lushchak, 2011). This process could result in physiological changes such as the immune system; causes decreased phagocytic activity or tissue and organ damage, and an inflammatory response such as program cell death, growth defects, and reduced reproductive ability. (Cheng & Sullivan, 1984; Yavasoglu et al., 2016). However, physiological changes in bivalves are a sign of alterations in the rates of filtration, feeding, growth, respiration, and reproduction. Guzmán-García and team (2008) reported that they monitor metal concentrations, including cadmium and lead in the Mandinga Lagoon in the Mexican State, which is affected by increased industrialization. The histopathological alteration in *Crassostrea virginica*, the digestive gland presented hyperplasia of epithelial cells in the tubules, the presence of brown vesicles, and an increase in hemocytes and necrosis correlated with environmental pollutants increased brown blood cell counts associated with inflammatory responses along with blood cell at the site of inflammation. These changes represent mechanisms of pollutants.

4. Risk assessment

Three main steps when responding to risk: Risk Assessment, Risk Management, and Risk Communication. These are shown in **Figure 1**.

4.1 Risk Assessment

Risk Assessment is the identification, analysis, and quantification of risk. This assessment determines the level of risk associated with a hazard, and four levels are commonly used: very high risk, high risk, medium risk, and low risk (Taylor, 2008). The four steps within Risk Assessment are described below.

4.1.1 Hazard Identification

The process of familiarization with the risk of a heavy metal or other hazard by researching its characteristics in previous literature.

4.1.2 Hazard Characterization

Describes dose-response assessment after human exposure. This is assessed from the relationship between the toxin levels of exposure and adverse effects on health.

4.1.3 Exposure Assessment

The process of carrying out quantitative and qualitative evaluations of heavy metal exposure, for example the degrees of seriousness depending on different exposures, and the residue levels that are harmful to health.

4.1.4 Risk Characterization

The last of the four steps of risk assessment. This integrates the data to analyze and summarize the probable risks and potential risks to consumers.

4.2 Risk Management

The process of forming risk data into guidelines. These guidelines should be practical and also very clear, in order to avoid misinterpretations. There are four steps within evaluation, as follows:

4.2.1 Risk evaluation

4.2.2 Development of risk management plan

4.2.3 Implementation of risk management plan

4.2.4 Monitoring and review

4.3 Risk Communication

The dissemination of information to the public on health risks and recommended actions. This enables people to make informed decisions for their safety and reduce anxiety related to the relevant risks.



Figure 1 Three main steps when responding to risk are: Risk Assessment, Risk Management, and Risk Communication (modified from Bekiari and Manoli, 2016).

CHAPTER III

METHODOLOGY

1. Study areas and *Saccostrea cucullata* collection

The hooded oyster *Saccostrea cucullata* was hand-collected from intertidal regions at two sites in Libong Island, Thailand. The Stone Bridge site ($7^{\circ}16'17.9''\text{N}$ $99^{\circ}22'38.3''\text{E}$) is the sand and stone beach, whereas the Dugong Tourism by Drones site ($7^{\circ}13'20.6''\text{N}$ $99^{\circ}24'08.3''\text{E}$) is close to the seagrass beds, as showed in **Figure 2**. Thirty-six individuals per site were collected and transported alive in polyethylene bags to the Histology Laboratory at the Medical Science Academic Service Centre under the laboratory quality standard (Number 2-0100-0004-8), Faculty of Medical Science, Naresuan University. All procedures were performed under the Naresuan University Animal Care and Use Committee under process number NU-AQ650303. The following water quality parameters were recorded using a portable water quality checker (HORIBA, Japan): dissolved oxygen (DO), water temperature (WT), salinity (S), total dissolved solids (TDS), and electrical conductivity (EC). The TDS and EC values were used to calculate the K value.

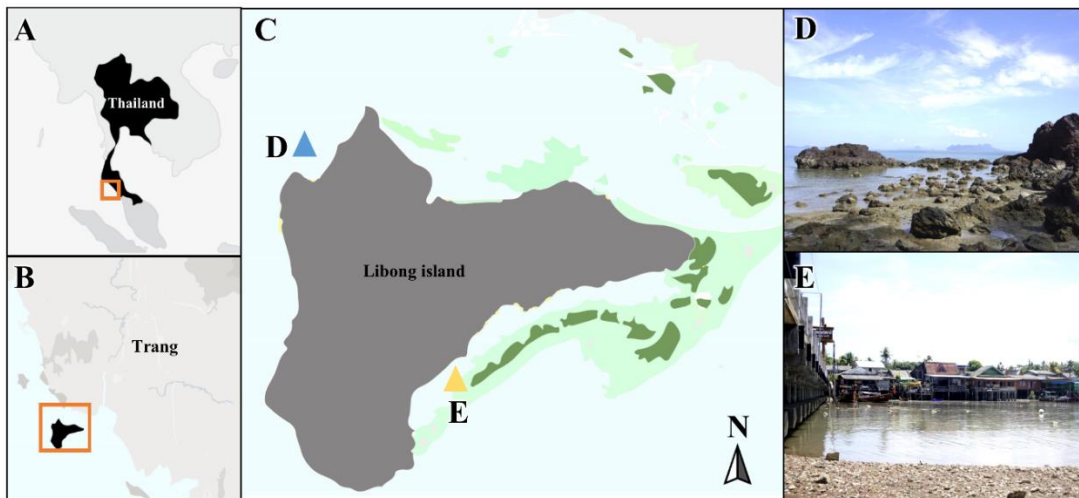


Figure 2 The sampling sites at Libong Island, Thailand. (A-B) Overview of Libong Island. (C-E) The two *Saccostrea cucullata*'s collection areas on this island include the Stone Bridge site (Blue head arrow, D) and the Dugong Tourism by Drones site (Yellow head arrow, E).

2. Morphometry and morphological examination

Morphometric measurements and gross anatomy examination of the *S. cucullata* were performed according to the standard methods of the OIE Diagnostic Manual for Diseases of Aquatic Animals (OIE, 2021). Species identification was based on major morphological characteristics of the oyster shell according to Cardoso et al. (2021). The shell length was measured from the longest axis of the shell to determine the size distribution using a vernier caliper to measure the shell height, shell length, and shell width to the nearest 0.01 mm, as showed in **Figure 3**. The soft tissue weight was also recorded using a digital scale to an accuracy of 0.01 g to assess the growth of this oyster. The condition factor (CF) was calculated to assess the general health condition and growth (Lim et al., 2020) using the following equation: $CF = 100W/L^3$, where W is the weight (g) and L is the total length (cm).

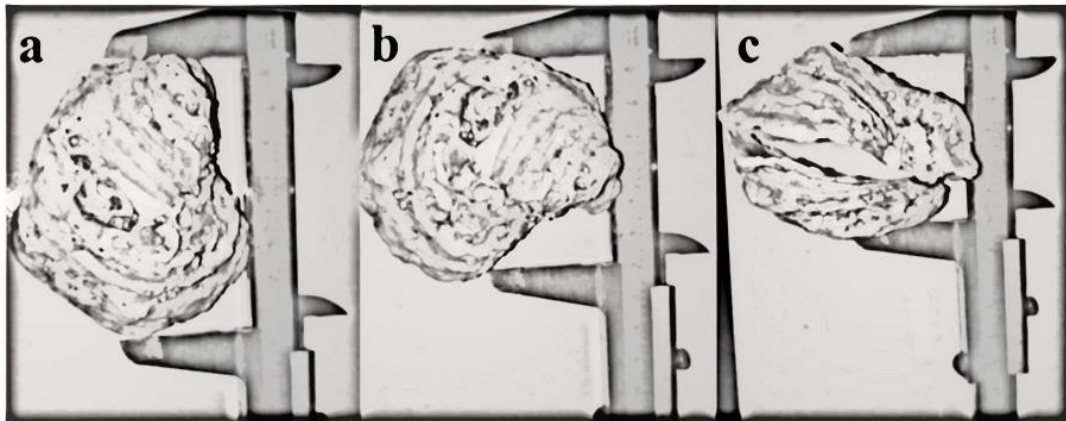


Figure 3 Morphometric measurement of the *S. cucullata*. Shell height (A), shell length (B), and shell width (C) all in millimeters (Cardoso et al., 2021)

3. Histological evaluations

The sampled *S. cucullata* were euthanized by a rapidly cooling shock and were separated into two groups for the histopathological analysis (n = 6 individuals per site) and measurement of heavy metal bioaccumulation (n=30 individuals per site; stored at -20 C). The samples in the first group were opened with an oyster knife by cutting the adductor muscle following the standard method (OIE, 2021). The samples were then dissected with a microtome blade, firstly at the gill-palp junction and secondly at 4 mm posterior to the first cut (Fig 4A-4B), followed by fixation in 10% neutral-buffered formalin fixative for 24 hr at room temperature. The fixed cross-sections were subjected to the decalcifying agent (Surgipath Decalcifier I) for 3 hr at room temperature and were processed by the standard histological technique (Fig 5A-5B, Table 1, Howard et al., 2004; Kongthong et al., 2022). The paraffin blocks were sectioned at 4 μ m thickness with a rotary microtome and stained with Masson's trichrome staining (MT, Fig 7) to observe histopathological alterations. The details of the histological slides were subjected to visual examination in **Table 2**. The multi-organ histopathological assessment (gills, digestive gland, gonads and mantle) was performed by visual examination using a light microscope and a PANNORAMIC Digital Slide Scanners (3DHISTECH) and histomorphometric evaluation using imageJ analysis (Fig 8). We also calculated the health assessment index (HAI) to assess the oyster health condition in the field using a modified protocol of Adams et al. (2010).

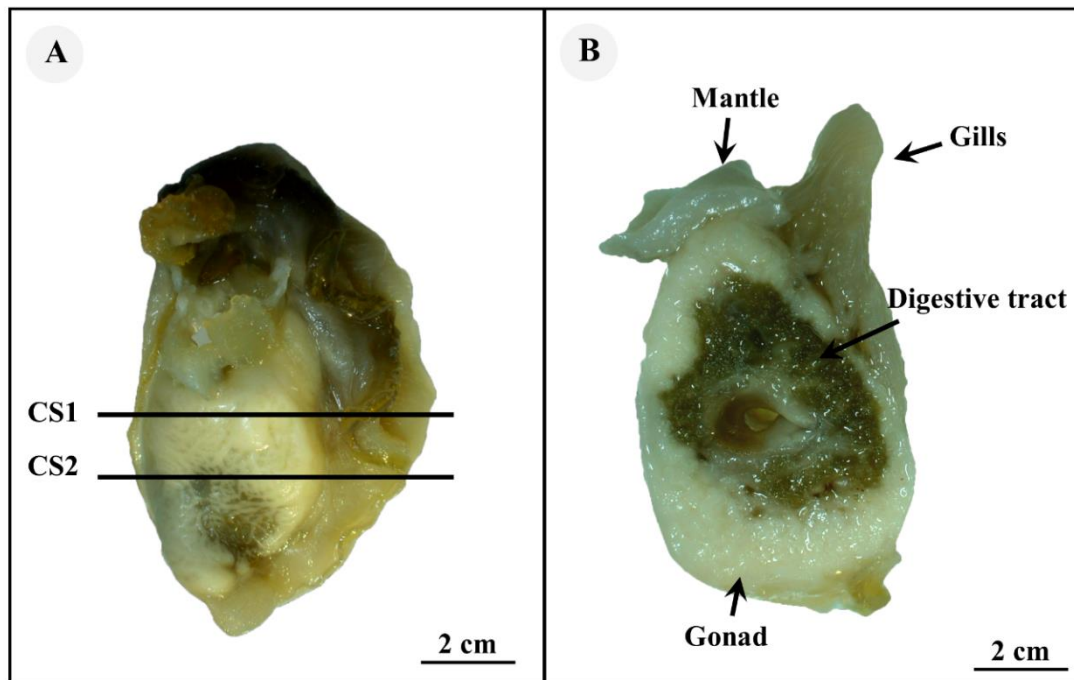


Figure 4 Hooded oyster, *Saccostrea cucullata*. (A) Transverse sections were collected (between the lines) by performing two plans with a Low-Profile Disposable Microtome Blade. (B) Gross anatomy of *S. cucullata*.

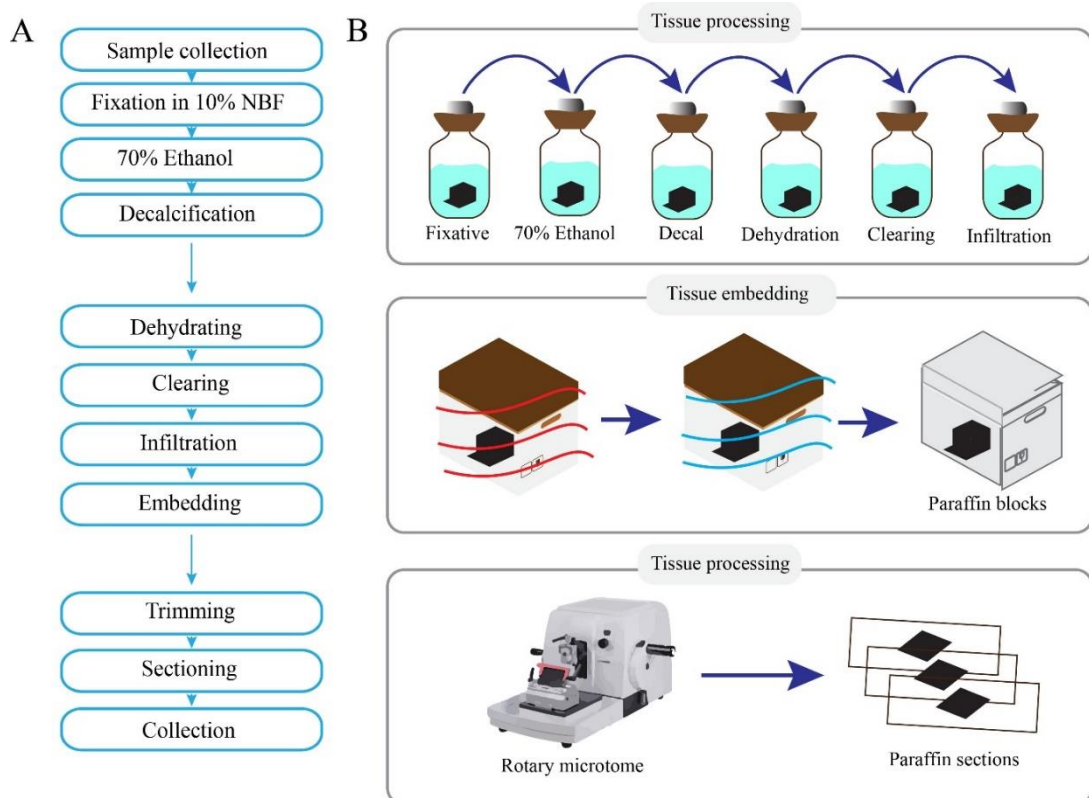


Figure 5 Schematic diagram for the entire experimental procedure. (A) Flowchart for the all steps of the protocol. (B) Schematic diagram illustrating the procedure for embedding large organs (take the macaque hemisphere as example, Kongthong et al., 2022).

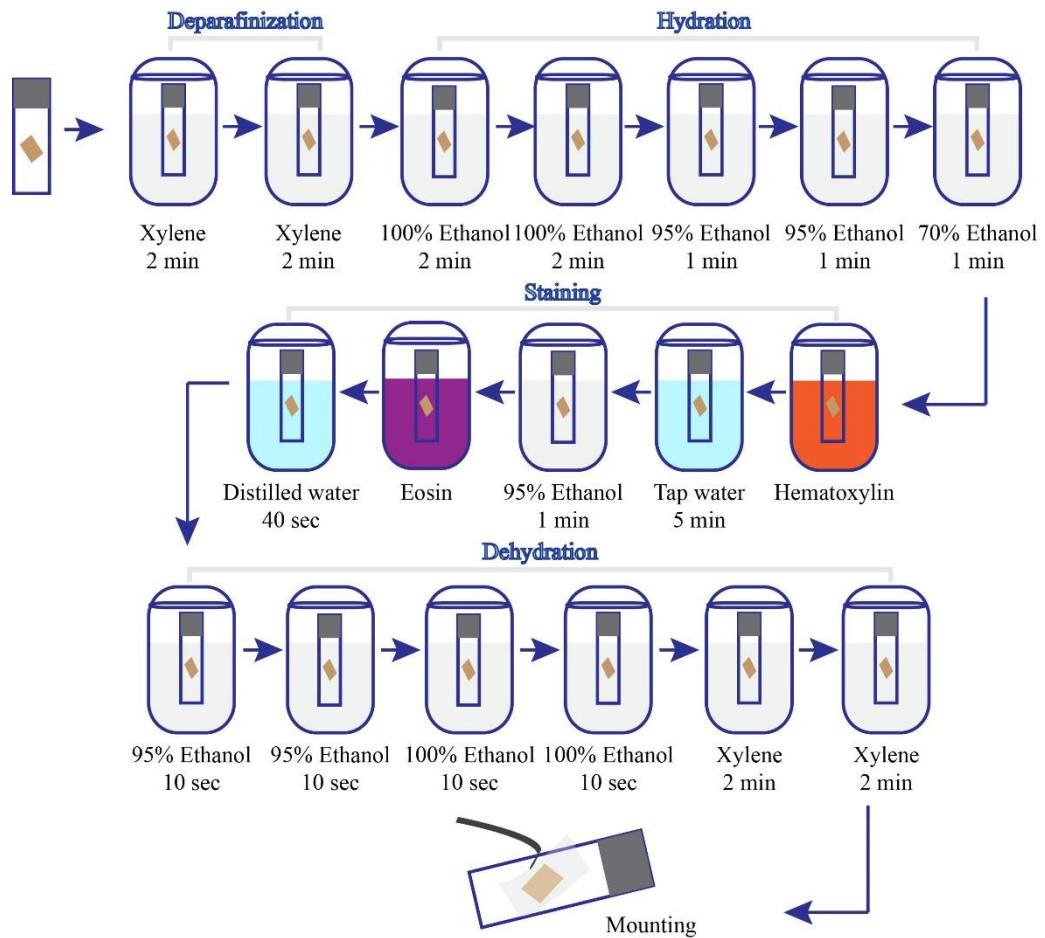


Figure 6 Schematic diagram for the entire experimental procedure showed Hematoxylin & Eosin staining protocol for *S. cucullata* samples (Kongthong et al., 2022)

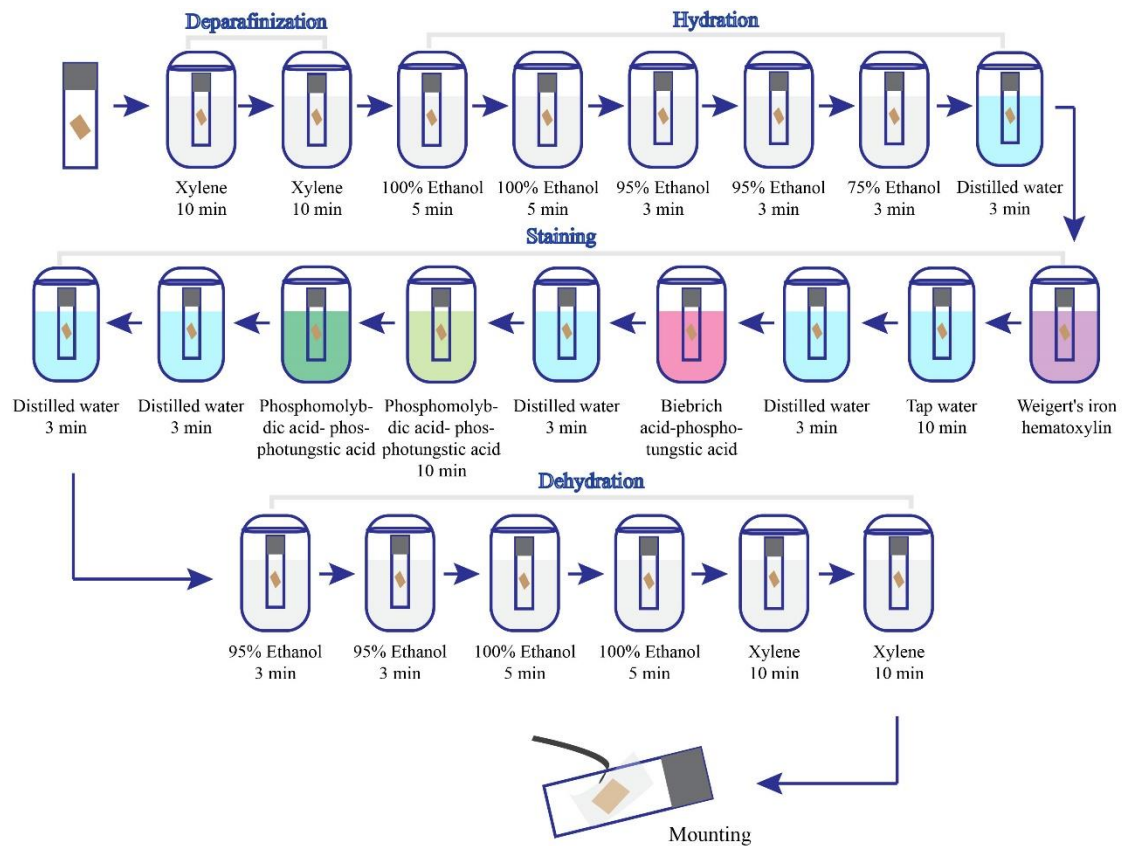


Figure 7 Masson's trichrome staining protocol for *S. cucullata* samples (Kongthong et al., 2022)

Table 1 The tissue processing protocol for *S. cucullata* samples

No.	Process	Time (min)
1	70% Alcohol	30
2	80% Alcohol	30
3	90% Alcohol	30
4	95% Alcohol I	90
5	95% Alcohol II	120
6	100% Alcohol I	120
7	100% Alcohol II	120
8	100% Alcohol III	120
9	Xylene I	90
10	Xylene II	120
11	Xylene : Paraplast (1:1)	60
12	Paraplast I	90

Source: Kongthong et al. (2022)

Table 2 Histological characteristics of *S. cucullata* observed in this study

Organs/Cells	Morphometric descriptions
Gill filament	The length of the gill lamellae from base to apex (n = 50 per individual sample of size distribution)
Mantle epithelium	The mantle epithelium (n=50 per individual sample of size distribution)
Digestive tubule	The diameter of primary ducts (n= 50 per individual sample of size distribution)
Mucous-secreting cell (Msc)	Types of mucous-secreting cells: oval, cup-shaped, pear-shaped, stick-shaped
Gametogenic cell and tissue	Types of germ cells: male, female, hermaphrodites, or asexual reproductive patterns Gametogenesis and gonadal maturation Oogenic differentiation

Source: Yonge (1926); Di et al. (2012); Zhang et al. (2019); García-Corona et al. (2018); Castilho-Westphal et al. (2013)

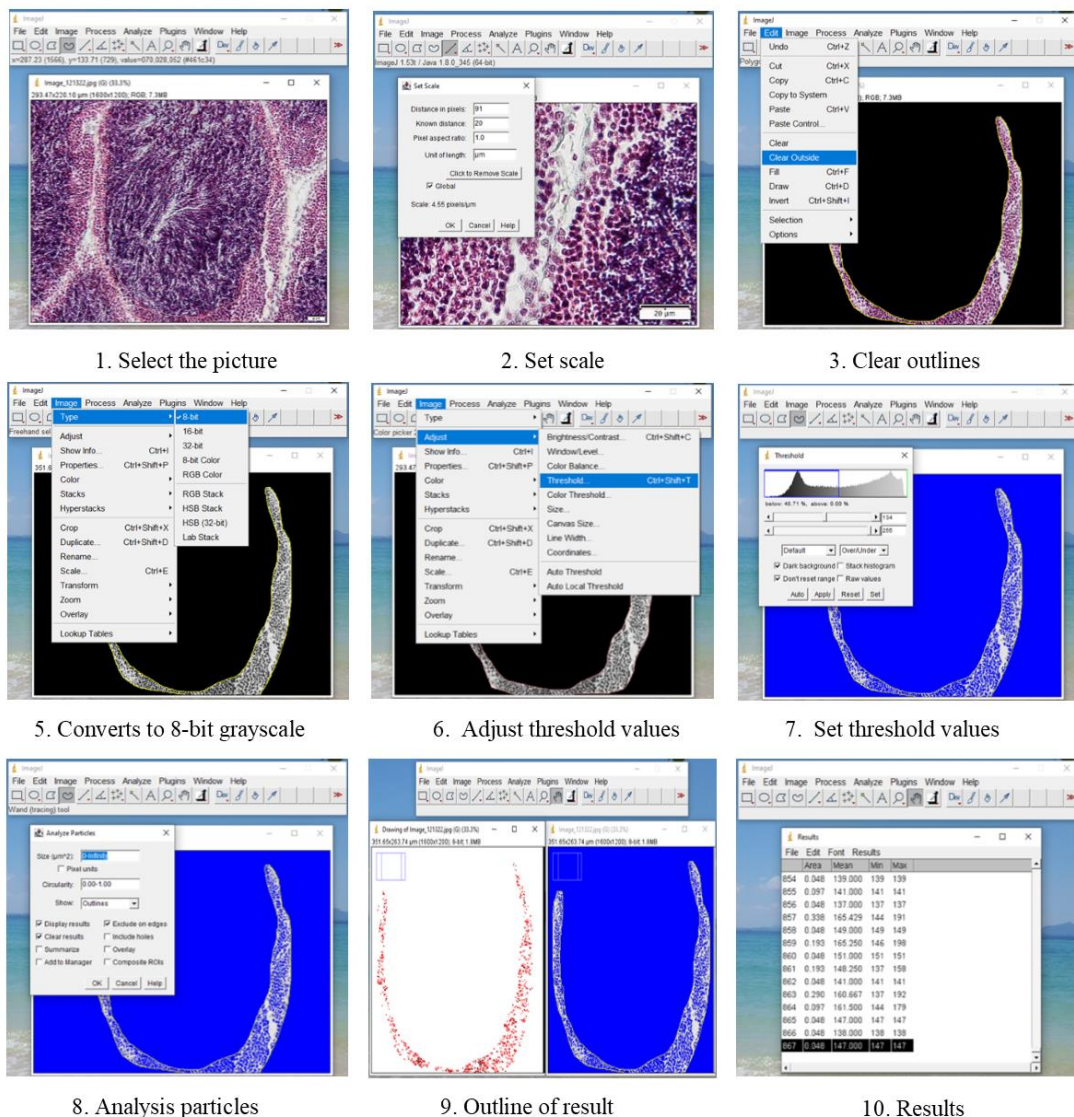


Figure 8 Digital image analysis process from ImageJ for the *S. cucullata*

4. In situ apoptosis detection using the TUNEL assay

The remaining unstained sections from the previous step were subjected to the TUNEL assay using an in situ TUNEL detection kit (Abcam, UK., Cat No: ab206386) according to the manufacturer's protocol. Briefly, the samples were deparaffinized in xylene, rehydrated in an ordered series of ethanol, rinsed with 1x Tris Buffered Saline (TBS) (pH 7.6), and then permeabilized by the proteinase K solution at room temperature for 20 min. All sections were submerged in 30% H₂O₂ at room temperature for 5 min for inactivation of endogenous peroxidases and rinsed with TBS. The samples were equilibrated with the TdT Equilibration Buffer at room temperature for 30 min

and incubated with TdT Enzyme in below 22 °C for 1.5 h in a humidified chamber, followed by termination of the enzymatic reaction using blocking buffer (10 min). The samples were incubated with horseradish peroxidase solution (HRP) for 30 min at room temperature. Finally, the slides were stained with the diaminobenzidine system (DAB) and counterstained with methyl green for 1-3 min. After counterstaining, the tissue sections were dehydrated in a graded series of ethanol, cleared in xylene, and mounted with permount media. The TUNEL-positive cells from the stained sections were analyzed using a light microscope and scanned with a PANORAMIC Digital Slide Scanner (3DHISTECH). The density of apoptotic cells was calculated by counting them at 40× magnification in specific areas. Apoptotic cells were subjected at 40× magnification and calculated area of the selective organ including gill lamellae (n=10 per individuals), digestive tubule (n = 50 tubules per individual), mantle (n=5 area per individuals), testis (n = 10 follicles per individuals) and ovary (n = 10 follicles per individuals) using ImageJ software. The percentage of TUNEL-positive cell density was then calculated based on the number of positive cells/the total number of cells (positive + negative) and the multiplication of the ratios by 100 (Ceylan & Kaptaner, 2019).

5. Heavy metal analysis

The selected organs of *S. cucullata* including gonads, digestive gland, gills, and mantle (n = 30 individual samples per area) were dissected and separated from the ventral side located the gills and mantles and inside is the digestive gland and gonadal organ. It is conducted according to the standard method from AOAC (2005). About 20 g of each organ were oven-dried at 105 °C for 48 h or until a constant weight. The resulting powdered organs of about 0.5 g of dry weight with three replicates (so total number of samples n = 3 per treatment) were ashed at 450 °C for 8 hr using a furnace (Carbolite RWF 11, US), for this process the sample was white/grey color. The digested samples were done by using 10 mL of di-acid mixture solution having a 1:1 ratio of concentrated HCl and HNO₃, evaporated on the hot plate between 120-150 °C for 30 min – 1 h. The final volume was adjusted as 50 mL in a volumetric flask, and the solution was filtered using a filter paper and transferred to a plastic bottle. The concentration of heavy metals including cadmium (Cd), Copper (Cu), Lead (Pb), and

Zinc (Zn) were analyzed using an atomic absorption spectrophotometry (AAS, Model PinAAcle 900 F, PerkinElmer, USA). The specific parameters used for each element are shown in **Table 3**. The standard recovery percentage of heavy metals ranged from 98.50–99.10%. All tests were displayed as Mean \pm Standard error ($X \pm SE$).

Table 3 AAS instrument parameters

Parameters	Zn	Cu	Cd	Pb
Wavelength (nm)	213.9	324.7	228.8	283.3
Detection limit (mg/l)	≥ 0.7	≥ 0.2	0.175	0.53

Source: Bekiari and Manoli (2016)

6. Human Health Risk Assessment (HRA)

We assessed the potential impact of the hooded oyster from Libong Island on human health using the human health risk assessment (HRA, Wuana et al., 2020). The hazard quotient (HQ), which first required determining the Chronic Daily Intake (CDI). The CDI was the daily dose of heavy metals (mg/kg-day) to which consumers might be exposed, and it was calculated with the following equation, using the input parameters defined in **Table 4**:

$$CDI = \frac{CS \times EF \times ED \times IR}{AT \times BW}$$

Table 4 Input parameters to calculate CDI

Factor/parameter	Symbol	Unit
Concentration of heavy metal in oyster	CS	Mg/kg
Exposure frequency	EF	360 days / years
Exposure duration	ED	30 days / years
Ingestion rate	IR	0.082 kg/day/person
Averaging time	AT	365 days / year*ED
Body Weight	BW	50 kg

Source: Denil et al. (2017), USEPA (2002)

Once the CDI was calculated, the hazard quotient (HQ) used following equation:

$$HQ = \frac{CDI}{Rfd}$$

Where: Rfd was the Reference Dose for Chronic Oral Exposure (mg / kg-day). The oral toxicity reference dose (RfD) values for the four heavy metals tested in this study are shown in **Table 5**.

Table 5 The oral reference dose (RfD) for the four heavy metals tested in this study

Heavy metal	Rfd (mg / kg per day)
Cadmium, Cd	0.001
Lead, Pb	0.0035
Copper, Cu	0.040
Zinc, Zn	0.3

Source: USEPA, 2011

The hazard quotient (HQ) is used to define 4 hazard risk levels, as showed in **Table 6**.

Table 6 HQ values and corresponding hazard risk levels

Index values	Degree of hazard
HQ < 0.1	Represents acceptable level
$0.1 \geq \text{HQ} \leq 1.0$	Low
$1.1 \geq \text{HQ} \leq 10$	Moderate
HQ > 10	Severe

7. Statistical analysis

7.1 The water quality parameters, morphometric observations, condition factors, the mucous-secreting cell (Msc) density, and gametogenic histology data that were represented as mean \pm SE. The unpaired t-test was used to compare these values between locations. The Msc and gametogenic histology data were subjected to Two-way ANOVA to determine statistical differences at $p < 0.05$.

7.2 The histopathological scores, the number of apoptotic cells, and the heavy metal concentrations were expressed as mean \pm SD. The histopathological score, density of apoptotic cells, and heavy metal concentrations were subjected to two-way ANOVA to detect significant effects of sampling sites and organs. The Bonferroni test and Welch's t-test were used as the post-hoc test. (GraphPad Prism for Windows version, R ver. 4.3.1).

CHAPTER IV

RESULTS

1. Water quality parameters

The water quality parameters including DO, pH, salinity, turbidity, TDS and EC were not significantly different between locations (Table 7), except for water temperature. The water temperature at the Dugong Tourism by Drones site was significantly higher than at Stone Bridge. The K values calculated from TDS and EC were 0.61 at both sites.

Table 7 The environmental factors between the sampling sites

Environment factors	Stone Bridge	Dugong Tourism by Drones	Standard Range
	mean±SE	mean±SE	
Dissolved Oxygen (m/L)	6.46±0.49	6.35±0.42	>5 mg/L
Water temperature (°C)	31.71±0.07*	33.73±0.90*	25–30 °C
pH	8.26±0.37	8.85±0.24	6.5–9.0
Salinity (ppt)	31.13±0.15	31.47±0.07	20-30 ppt
Turbidity (NTU)	0.00	22.67±4.52	40 NTU
Depth (m)	0.88±0.09	0.78±0.12	-
Total Dissolved Solids: TDS (g/L)	29.17 ± 0.12	29.47 ± 0.07	-
Electrical Conductivity: EC (ms/cm)	47.83 ± 0.20	48.30 ± 0.10	-
K ratio between TDS and EC	0.61	0.61	≥0.7

Note: Values are represented as mean±SE (n=3). Significant differences between two locations (* p <0.05). SE, Standard Error; ppt, part per thousand; NTU, Nephelometric Turbidity Unit.

Source of the standard range: Howard et al. (2004); Rusydi (2018)

2. Shell size distribution in relation to histological development

The shell size distribution of *S. cucullata* was classified into five groups based on the shell length: 1-2, 2.1-3, 3.1-4, 4.1-5 and 5.1-6 cm (Table 8). The oysters from the Stone Bridge area were generally smaller than those from Dugong Tourism by Drones (Table 8). The highest and lowest mean condition factors (CF) were found in the size group of 1-2 cm (6.31 ± 1.67) and 5.1-6 cm (0.95 ± 0.48) from Dugong Tourism by Drones, respectively (Table 9). In the size groups of 2.1-3 to 4.1-5 cm, the mean condition factors were higher in individuals from the Stone Bridge than those from Dugong Tourism by Drones. Under panoramic figures, several organizations including the digestive gland, gills, and mantle epithelium tissue were histologically identified (Fig. 8A).

The digestive gland (or hepatopancreatic tissue) was composed of several blind-ended tubules, each of which could be divided into the primary and secondary ducts (Fig. 8B). The primary ducts were connected to the stomach wall (Fig. 8B). The smallest and largest primary ducts were $105.4 \pm 3.03 \mu\text{m}$ in the 1-2 cm size group and $139.9 \pm 3.63 \mu\text{m}$ in the 5.1-6 cm size group, respectively, both of which were observed in *S. cucullata* from the Dugong Tourism by Drones. However, there were no significant differences in the average diameter of the primary and secondary ducts between *S. cucullata* from the two locations.

The gills structure of *S. cucullata* was made of V-shaped demi-branches, which were clearly separated by the central axis (Fig. 8C). Each short gill filament extended toward either side of the axis, and the cilia observed on their surfaces were expected to produce the respiratory current (Fig. 8C). The gill filaments were divided into two rows and three zones, including the frontal, intermediate, and abfrontal zones (Fig. 8C). The anterior surface of the gill filament was covered with the cilia (Fig. 8C). The longest gill lamellae was observed in *S. cucullata* from the Dugong Tourism by Drones ($280.2 \pm 7.90 \mu\text{m}$ in the 5.1–6 cm size group), whereas the shortest was recorded in the 3.1–4 cm group from the Stone Bridge ($127.8 \pm 3.29 \mu\text{m}$, Table 2). It was interesting that the mean lengths were significantly different between locations (Table 8).

The mantle of *S. cucullata* was covered with the vesicle mass, which histologically consisted of two epithelium layers including outer epithelium and inner

epithelium separated by haemolymph sinuses and connective tissues (Fig. 8D). Both the thickest ($31.24 \pm 3.03 \mu\text{m}$ in the 1-2 cm group) and thinnest ($73.78 \pm 3.08 \mu\text{m}$ in the 4.1-5 cm group mantle epithelia were found in *S. cucullata* from Dugong Tourism by Drones (Table 8). The lengths of mantle epithelium were significantly different between the 4.1-5 cm size groups from the two locations (Specific F value= 0.8605, $p < 0.0001$).

Table 8 Morphometric measurement based on the different sizes of *S. cucullata* between Stone Bridge and Dugong Tourism by Drones site

Size	Stone Bridge			Dugong Tourism by Drones		
	Diameter of digestive tubules (μm)	Length of gills (μm)	Length of mantle epithelium (μm)	Diameter of digestive tubules (μm)	Length of gills (μm)	Length of mantle epithelium (μm)
1-2 cm	-	-	-	105.4 ± 3.03	152.3 ± 5.46	31.24 ± 3.03
2.1-3 cm	120.9 ± 3.18	$127.8 \pm 3.29^{***}$	45.27 ± 3.18	121.9 ± 3.81	$192.1 \pm 3.92^{***}$	43.62 ± 3.81
3.1-4 cm	126.9 ± 2.66	$145.7 \pm 4.33^{**}$	45.51 ± 2.66	112.8 ± 2.98	$157 \pm 3.21^{**}$	45.05 ± 2.98
4.1-5 cm	129.3 ± 2.93	181.2 ± 8.45	$60.72 \pm 2.93^{***}$	133 ± 3.08	172.2 ± 5.62	$73.78 \pm 3.08^{***}$
5.1-6 cm	-	-	-	139.9 ± 3.63	280.2 ± 7.90	67.07 ± 3.63

Note: Values are represented as mean \pm SE (n=6). Significant differences between Stone Bridge and Dugong Tourism by Drones (** $p < 0.01$; *** $p < 0.0001$).

Table 9 The condition factor (g/cm^3) of the sampled *S. cucullata* between Stone Bridge and Dugong Tourism by Drones site

Size distribution	Number of individuals	Stone Bridge	Dugong Tourism by Drones
		mean \pm SE	mean \pm SE
1-2 cm	10	-	6.31 \pm 1.67
2.1-3 cm	10	4.25 \pm 2.18	2.01 \pm 0.82
3.1-4 cm	10	3.93 \pm 1.41	2.16 \pm 0.68
4.1-5 cm	10	2.01 \pm 0.46	1.27 \pm 0.45
5.1-6 cm	10	-	0.95 \pm 0.48

Note: Values are represented as mean \pm SE (n =10). SE, Standard Error.

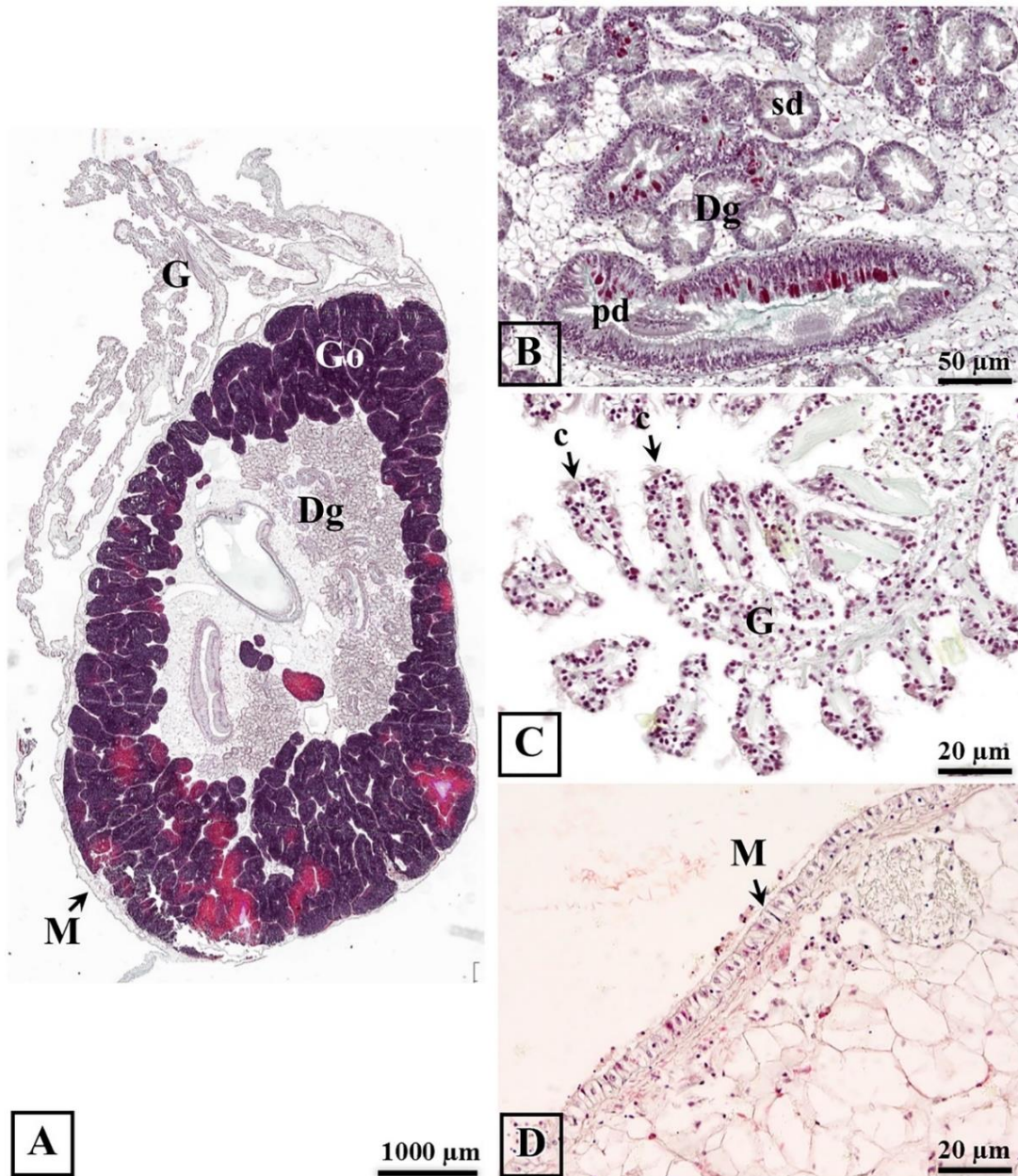


Figure 9 Histological observations of different tissues of *S. cucullata*. (A) The cross-section of *S. cucullata* showed the position of the digestive gland, gills, and mantle epithelium tissue. (B) Digestive gland histology showed the primary and secondary ducts. (C) Gill filaments extended toward the side; the cilia were observed on their surface. (D) The mantle layer in the vesicle mass with the connective tissue. Abbreviations: Dg, Digestive gland; pd, primary ducts; sd, secondary ducts; G, Gills; c, cilia; M, Mantle; Go, Gonad.

The gonadal follicles contained reproductive cells and developed in the vesicle mass (Fig. 9A). The gonads of *S. cucullata* revealed to be protandric from the 1-2 cm size group (Table 10). The male gonads were firstly formed with the blind-end testicular follicles containing spermatogonia (46.0 ± 24.54 cells of 2.1-3 cm at Stone Bridge)(Fig. 9B, Table 10). Primary spermatocytes, secondary spermatocytes, spermatids, and spermatozoa were also identified in the 1-2 cm size group from Stone Bridge (Figs 9C-9D, Table 10), and there was a tendency that male reproductive cells were more differentiated in larger size groups (Table 10). No significant differences in the number of spermatogenic cells were found between *S. cucullata* from Stone Bridge and Dugong Tourism by Drones site.

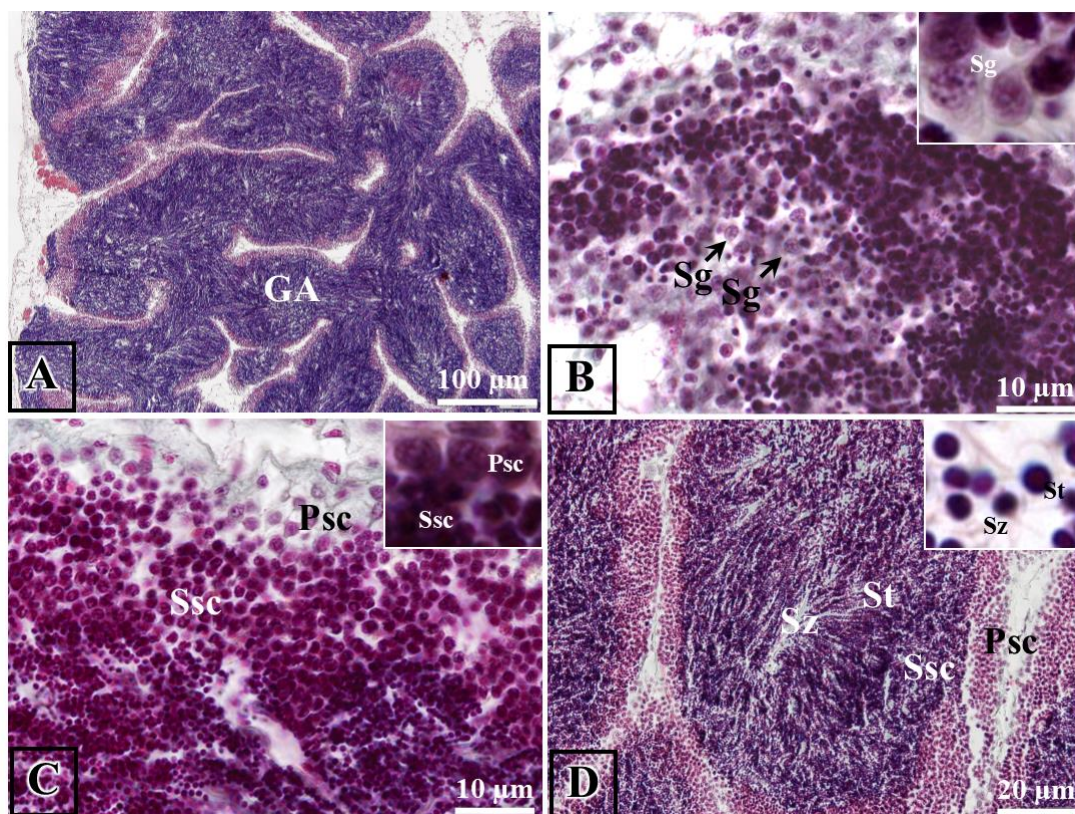


Figure 10 Light microscope observation of the male gonad of *S. cucullata*. The spermatogenesis was observed in the visceral mass. (A) The mature gonad in gonadal acini (GA), (B) and spermatogonia (arrow). (C-D) The gonadal acin contained primary spermatocytes, secondary spermatocytes, Spermatids and spermatozoa. Abbreviations: Sg, Spermatogonia; Psc, Primary spermatocytes; Ssc, Secondary spermatocytes; St, Spermatids; Sz, Spermatozoa.

Table 10 Type of male gonad of the *S. cucullata* from Stone Bridge and Dugong Tourism by Drones site

Locations	Size distribution	Number of individuals	Spermatogenesis stage				
			Spermatogonia (cells)	Primary spermatocytes (cells)	Secondary spermatocytes (cells)	Spermatids (cells)	Spermatozoa (cells)
Stone Bridge	2.1-3 cm	6	46.0±24.54	434.67±82.96	272.0±161.7	632.0±378.60	524.7±412.6
	3.1-4 cm	6	6.67±4.18	103.3±59.83	230.3±126.0	216.7±18.98	506.7±45.08
	4.1-5 cm	6	9.67±3.76	479.3±88.37	602.0±192.3	559.7±126.4	1306.0 ± 295.4
Dugong Tourism by Drones	1-2 cm	6	12.67±5.24	49.33±3.67	49.67±6.69	40.33±9.94	15.33±5.04
	2.1-3 cm	6	19.67±0.67	133.7±29.36	145.7±43.35	292.3±72.26	143.7±23.84
	3.1-4 cm	6	9.67±5.21	177.7±45.04	301.7±179.0	345.0±183.0	201.0±54.67

Note: Values are represented as mean±SE (n=6). No significant difference between Stone Bridge and Dugong Tourism by Drone areas ($p > 0.05$).

3. Gonad development

Undeveloped female gonads were observed in the 1-2 cm size groups. The ovary was histologically surrounded by a thin acini wall and contained developing oocytes (Figs 10A- 10B), which were classified into oogonia, immature oocytes, maturing oocytes, and mature oocytes (Table 11). Oogonia was prominently observed in the 2.1-3 cm size group (6.67±2.40 cells) from Dugong Tourism by Drones (Fig. 10B, Table 12). Immature oocytes had a polyhedral-shaped nucleolus at the peripheral area (9.67±2.33 cells of 4.1-5 cm at Stone Bridge) (Table 12). The mature oocytes had a polyhedral-shaped voluminous nucleus surrounded by the basophilic cytoplasm (9.0±0.58 cells of 4.1-5 cm at Stone Bridge) (Figs 10C-10D, Table 12) and completed in the spent stage. The development of mature oocytes was still seen, but the stromal compartment as well as the loose connective tissue was also increased (Figs 10E-10F, Table 12). However, no statistically significant differences in the ovarian activity were found between *S. cucullata* from Stone Bridge and Dugong Tourism by Drones site.

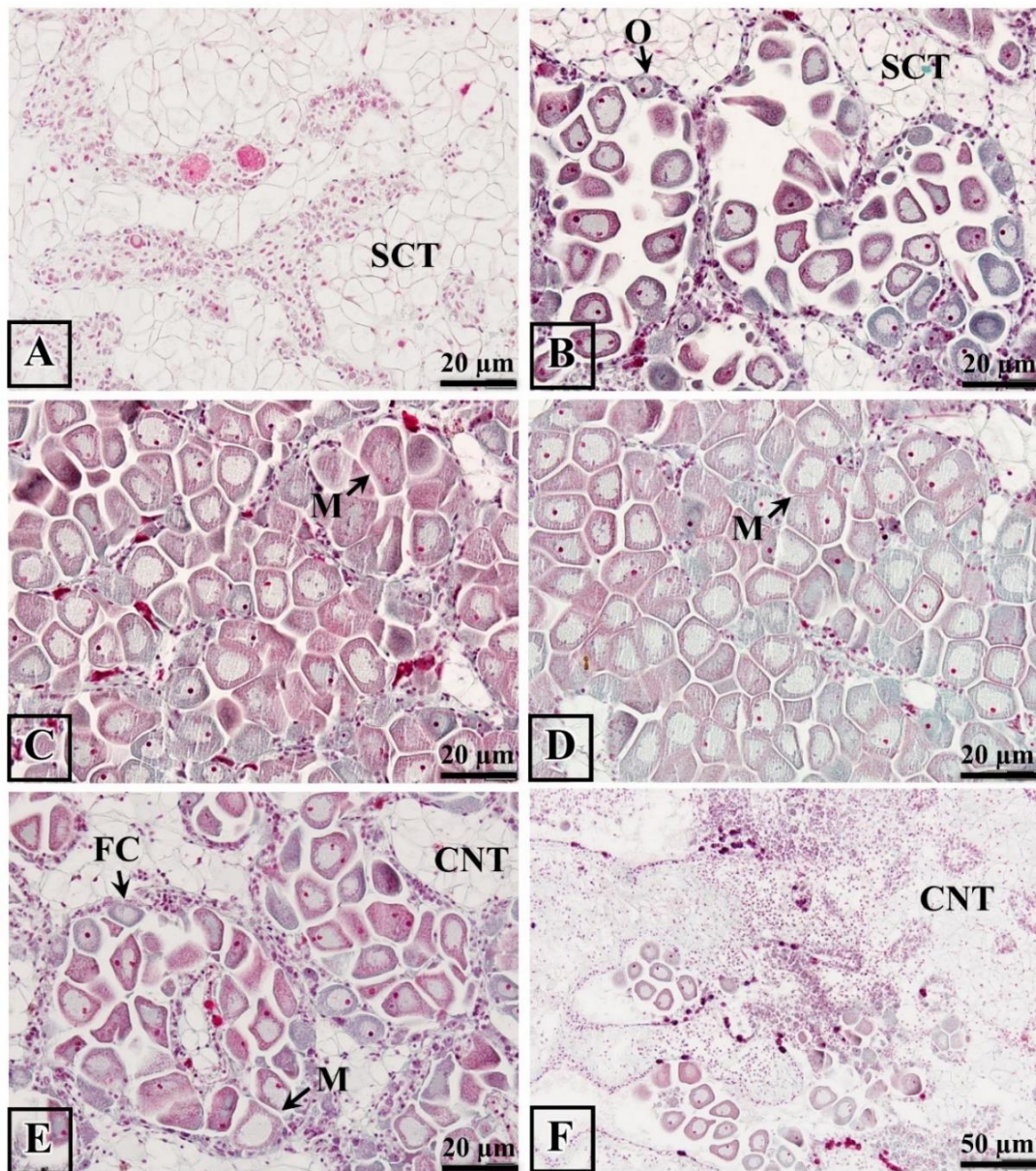


Figure 11 Light microscope showed the female gonad development of the *S. cucullata* in follicle. (A) Oocytes in pre-maturation stage with immature oocytes that stored connective tissue. (B) Mature oocytes can be found in the follicles. (C- D) The mature stage contained many mature oocytes and absent the interstitial tissue. (E-F) Mature oocytes in the spent stage and surrounded by follicular cells.

Abbreviations: SCT, Storage Connective Tissue; FC, Follicular Cells; O, oogonium; M, mature oocyte; CNT, Connective Tissue.

Table 11 The characteristics of spermatogenesis stage and oogenesis stage of the *S. cucullata*

Stage	Cells	Description
Spermatogenesis stage		
1	Spermatogonia	Large nucleus with distributed chromatin inside the cell
2	Spermatocytes	The nucleus condenses in the primary phase and through cell division in the secondary phase
3	Spermatids	Occurs from meiosis division in half of the genetic material of the previous cell, resulting in a reduced cell size and more compacted nuclei
4	Spermatozoa	Characterised by long flagella
Oogenesis stage		
1	Oogonia	The cytoplasm is reduced to the size of the nucleus of the basophil cell.
2	Immature oocytes	Basophils usually have a peripheral polyhedral-shaped nucleolus
3	Maturing oocytes	Lightly eosinophilic, polyhedral-shaped voluminous nucleus
4	Mature oocytes	Eosinophilic, voluminous nucleus, located near the follicle lumen

Table 12 Oocyte development in four stages of *S. cucullata* between two sites study

Size	Number of individuals	Stone Bridge				Dugong Tourism by Drones			
		Oogonia (cells)	Immature oocyte (cells)	Maturing oocytes (cells)	Mature oocyte (cells)	Oogonia (cells)	Immature oocyte (cells)	Maturing oocytes (cells)	Mature oocyte (cells)
1-2 cm	6	-	-	-	-	-	-	-	-
2.1-3 cm	6	5.33±1.76	5.0±1.0	5.67±1.20	7.667±1.20	6.67±2.40	1.33±0.33	0	0
3.1-4 cm	6	3.33±0.88	6.0±1.73	6.33±2.91	1.67±1.20	5.33±3.33	9.0±1.73	5.0±0.58	6.0±1.16
4.1-5 cm	6	2.0±1.16	9.67±2.33	9.0±0.58	10.67±1.76	1.33±0.33	2.67±0.88	2.67±0.88	4.67±0.88
5.1-6 cm	6	-	-	-	-	2.33±0.33	3.33±0.88	5.33±2.02	7.67±1.76

Note: Values are represented as mean±SE (n=6). No significant difference between Stone Bridge and Dugong Tourism by Drones areas ($p>0.05$).

Overall, *S. cucullata* individuals were primarily asexual in the smallest size group of 1-2 cm. The protandric characteristic appeared in the 2.1-3 cm and 3.1-4 cm size groups with observed sexes of female, male, and hermaphrodites. All of *S. cucullata* individuals in the 4.1-5 cm size group from Dugong Tourism by Drones site were female (Table 13).

Table 13 Percentage of sex difference of the *S. cucullata* between two locations

Size	Number of individuals	Stone Bridge				Dugong Tourism by Drones			
		Female	Male	Hermaphrodite	Asexual	Female	Male	Hermaphrodite	Asexual
1-2 cm	6	-	-	-	-	-	16.67%	-	83%
2.1-3 cm	6	50%	50%	-	-	50%	33.33%	-	16.67%
3.1-4 cm	6	50%	16.67%	33.33%	-	50%	33.33%	16.67%	-
4.1-5 cm	6	66.67%	16.67%	16.67%	-	100%	-	-	-
5.1-6 cm	6	-	-	-	-	100%	-	-	-

4. Distribution of mucous-secreting cells

The mucous-secreting cells (Msc) of *S. cucullata* had various shapes including oval, cup-like, stick-like, and pear-like shapes (Fig. 11A). In gill lamellae, Msc of the stick and cup shapes were observed (Fig. 11B); the digestive ducts contained those of oval and cup-like shapes (Fig. 11C); and mantle epithelium contained Msc of oval and pear shapes (Fig. 11D). Cup-like and oval-shaped cells were predominant (Fig. 11C) especially in the 3.1-4 cm size group from Stone Bridge (65.0 ± 44 cells).

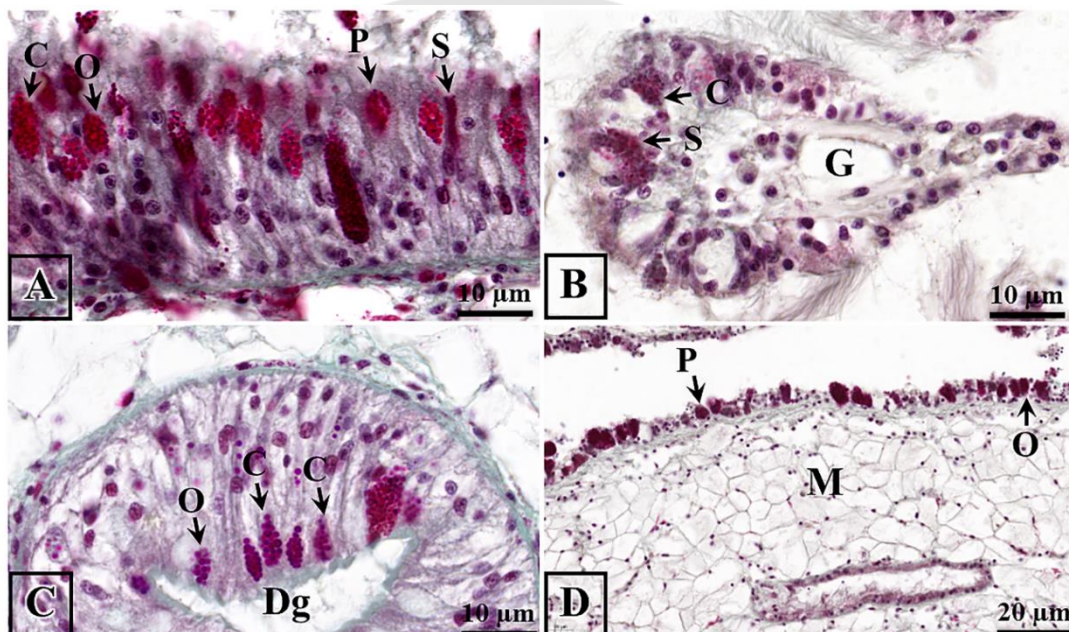


Figure 12 The light microscope of mucous-secreting cells of the *S. cucullata*. Masson's trichome staining. (A) Cross section of *S. cucullata* presented mucous-secreting cells in four types. (B) Mucous cells in gill filament with cup-like and stick-like shapes (arrow). (C) The secondary digestive tubules show mucous cells of oval and cup shapes (arrow). (D) Mantle epithelium cells show large mucous cells. Abbreviations: O, Oval or circle-like; C, cup-like; S, Stick-like; P, Pear-like.

Our investigation showed that increases in Msc were usually attributed to those in the gill lamellae having the oval, cup-like, and pear-like shapes (Fig. 11B). The density of Msc was lower in *S. cucullata* from Stone Bridge in the 4.1-5 cm size group (13.75 ± 9.20 cells) than the same size group from Dugong Tourism by Drones (37.50 ± 34.18 cells). For this study, we observed in the size group of 3.1-4 cm for *S.*

cucullata that its highest density of Msc from Stone Bridge (65.0 ± 44.75 cells) was observed in the digestive gland; however, it showed in the mantle epithelium (24.25 ± 11.32 cells) from Dugong Tourism by Drones. The smallest and largest Msc were recorded in the 4.1-5 cm size group from both locations (Table 14). Overall, our observation showed that the features of Msc were not significantly different between two locations (Table 14).

Table 14 Density of mucous-secreting cells in three tissue of the *S. cucullata* between Stone Bridge and Dugong Tourism by Drones site

Size	Stone Bridge			Dugong Tourism by Drones		
	Digestive gland (cells)	Gills (cells)	Mantle epithelium (cells)	Digestive gland (cells)	Gills (cells)	Mantle epithelium (cells)
1-2 cm	-	-	-	37.0±20.88	26.0±17.87	9.75±5.53
2.1-3 cm	32.50±24.52	15.75±11.81	9.00±4.56	23.25±8.34	35.75±28.24	17.00±9.55
3.1-4 cm	65.0±44.75	20.75±12.29	6.25±3.71	25.25±13.46	20.25±9.39	18.00±8.85
4.1-5 cm	27.25±13.15	13.75±9.20	5.75±2.75	39.75±27.93	37.50±34.18	24.25±11.32
5.1-6 cm	-	-	-	19.0±10.66	36.50±21.64	7.75±4.51

Note: Values are represented as mean±SE (n=6). No significant difference in between Stone Bridge and Dugong Tourism by Drones areas ($p>0.05$).

5. Histology and histopathological alteration of *S. cucullata*

The structure and histopathology of the digestive tubules, gill lamellae, mantle epithelium, testis, and ovary of *S. cucullata* were observed in samples from both sites (Fig. 12).

5.1 The digestive gland or hepatopancreatic tissue was composed of several blind ducts (Fig. 12A), each of which was connected to the stomach. Various histopathological alterations were observed in this organ, including the tubule regression, epithelium atrophy, and necrosis (Fig. 12A). Apoptotic cells were also found in the epidermal duct (Fig. 12B).

5.2 Gill lamellae was characterized by the V-shaped demi-branches, and each branch was lined by the stratified epithelium (Fig. 12C). Lamellae fusion and hemocytic infiltration were seen throughout the gill (Fig. 2C). In the gill epithelium, apoptotic cells were clearly observed with strong positive staining (Fig. 12D).

5.3 The mantle epithelium of *S. cucullata* was composed of two major structures including outer epithelium and inner epithelium. The lipid vacuole and the nuclear degeneration were identified in the inner epithelium (Fig. 12E). The positive reaction was observed in the TUNEL assay in the nuclei of epithelium, indicating the apoptosis (Fig. 12F).

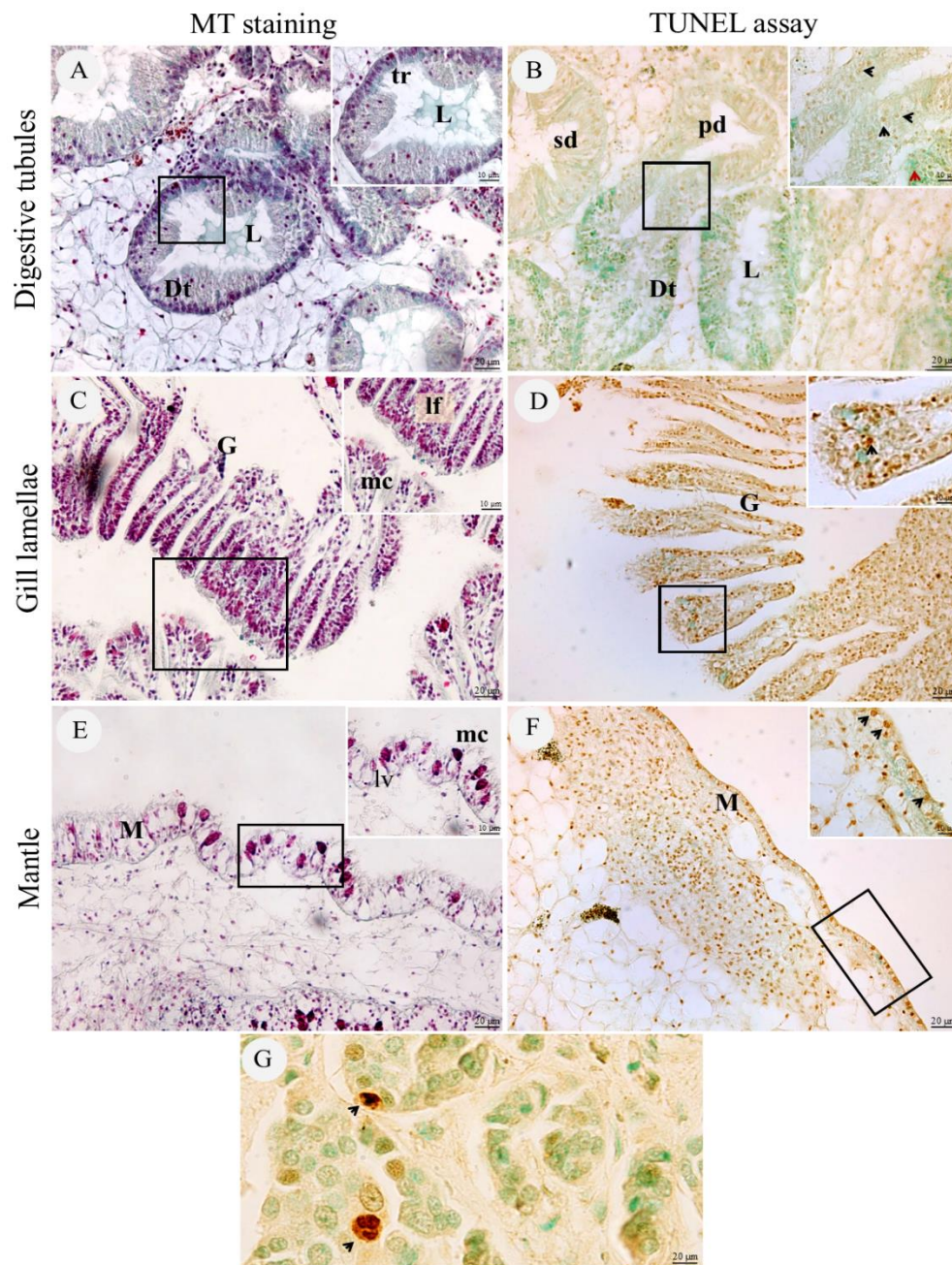


Figure 13 Histopathological alteration and the presence of apoptotic cell in the of the *S. cucullata* tissue between the Stone Bridge and the Dugong Tourism by Drones site. (A-B) Digestive tubules regression with the appearance of apoptotic cell in the digestive epithelium (head arrows). (C-D) Gill lamellae fusion and hemocytic infiltration as well as the presence of apoptotic cell (head arrows). (E-F) Lipid vacuoles and mucocytes in the mantle epithelium throughout the visible of apoptotic cell (head arrows). (G) TUNEL-positive control. Abbreviations: Dt = Digestive tubule, tr = tubules regression; pd = primary ducts; sd = secondary ducts, L = Lumen, G = Gill lamellae, lf = lamellae fusion, M = Mantle epithelium, mc = mucous cells, lv = lipid vacuole

5.4 The gonadal acini having the reproductive cells were observed in the reproductive parenchyma. Several reproductive follicles were identified in the testis and ovary (Representative Fig. 13A-13D). The testicular parenchyma produced spermatozoa, and spermatids and spermatocytes were localized close to the follicular membrane (Fig. 13A). The syncytium of spermatozoa (Fig. 13A) and the vacuolar degeneration of previtellogenic oocyte were observed (Fig. 13I). Several TUNEL-positive reactions were found as shown in Fig. 13B and 13D.

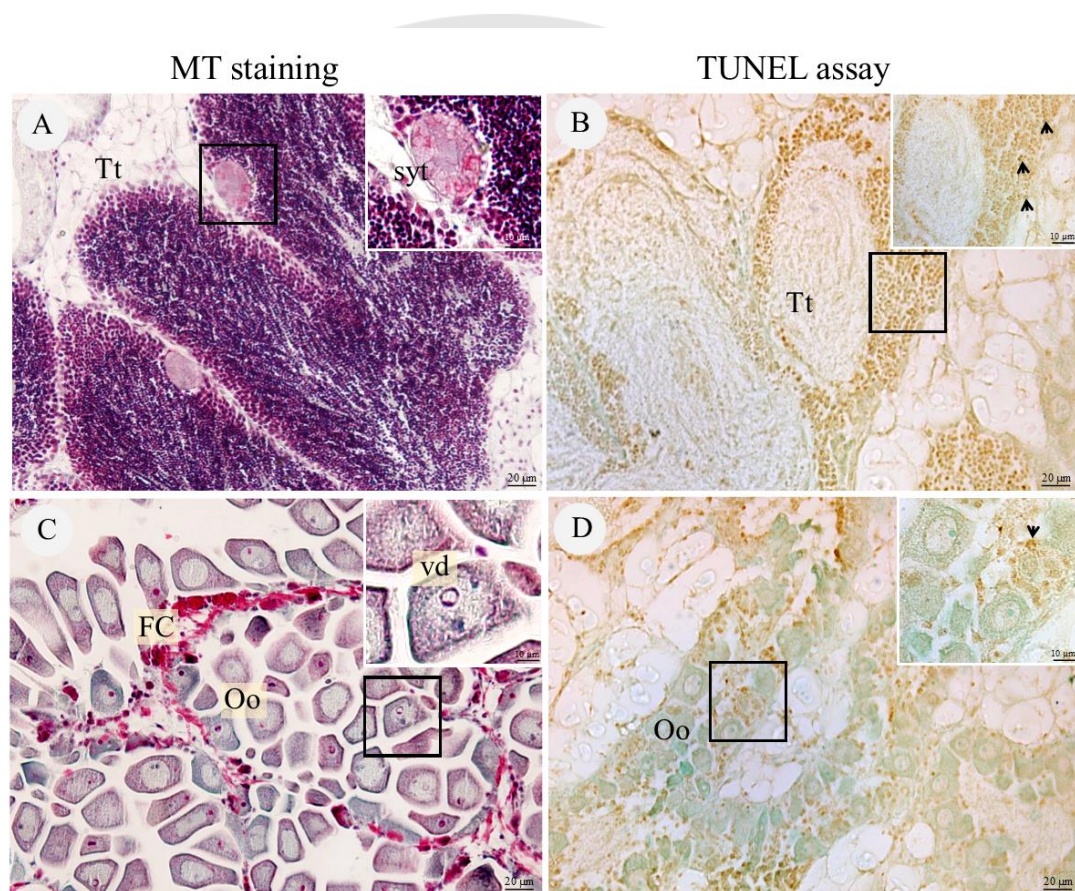


Figure 14 A photomicrograph of reproductive organ of the *S. cucullata* collected from the Stone Bridge and Dugong Tourism by Drones. (A) The histopathological lesion of the testicular showed the syncytium of spermatozoa and (B) TUNEL- positive were also observed at high magnification (100x, arrow). (C) Ovarian contained the oocytes with the vacuolar degeneration (Vd) at higher magnification and (D) black arrowheads was signifying the dark brown expression of TUNEL-positive cells. Abbreviations: Tt = Testis, syt = syncytium of spermatozoa, Oo = Oocytes, FC = Follicle Cells, vd = vacuolar degeneration

The HAI and the percentage of apoptotic cells were compared between the two sampling sites (Fig. 14A). Samples from the Dugong Tourism by Drones site generally had higher HAI. Significant differences between the two sites were found in the epithelial atrophy and tubular regression of the digestive gland as well as hemolytic infiltration and the presence of mucous cells in the gill lamellae (Fig. 13A). The density of apoptotic cells was statistically analyzed by two-way ANOVA for the effect of organs and sampling sites in the gill, digestive gland, and mantle epithelium. The effect of organs was statistically significant ($df = 3, F = 46.2, p < 0.0001$). The effect of sampling sites was not significant ($df = 1, F = 0.002, p = 0.97$), but there was a strong interaction between the two factors ($p < 0.0001$) that indicates the different responses of each organ to environmental stress. Specifically, gill showed a markedly higher percentage of apoptotic cells, which was significantly higher in *S. cucullata* from the Dugong Tourism by Drones compared to those from the Stone Bridge site (Fig. 14B). Significant differences were also detected in digestive tubules and gonads, for which samples from the Stone Bridge site showed higher values.

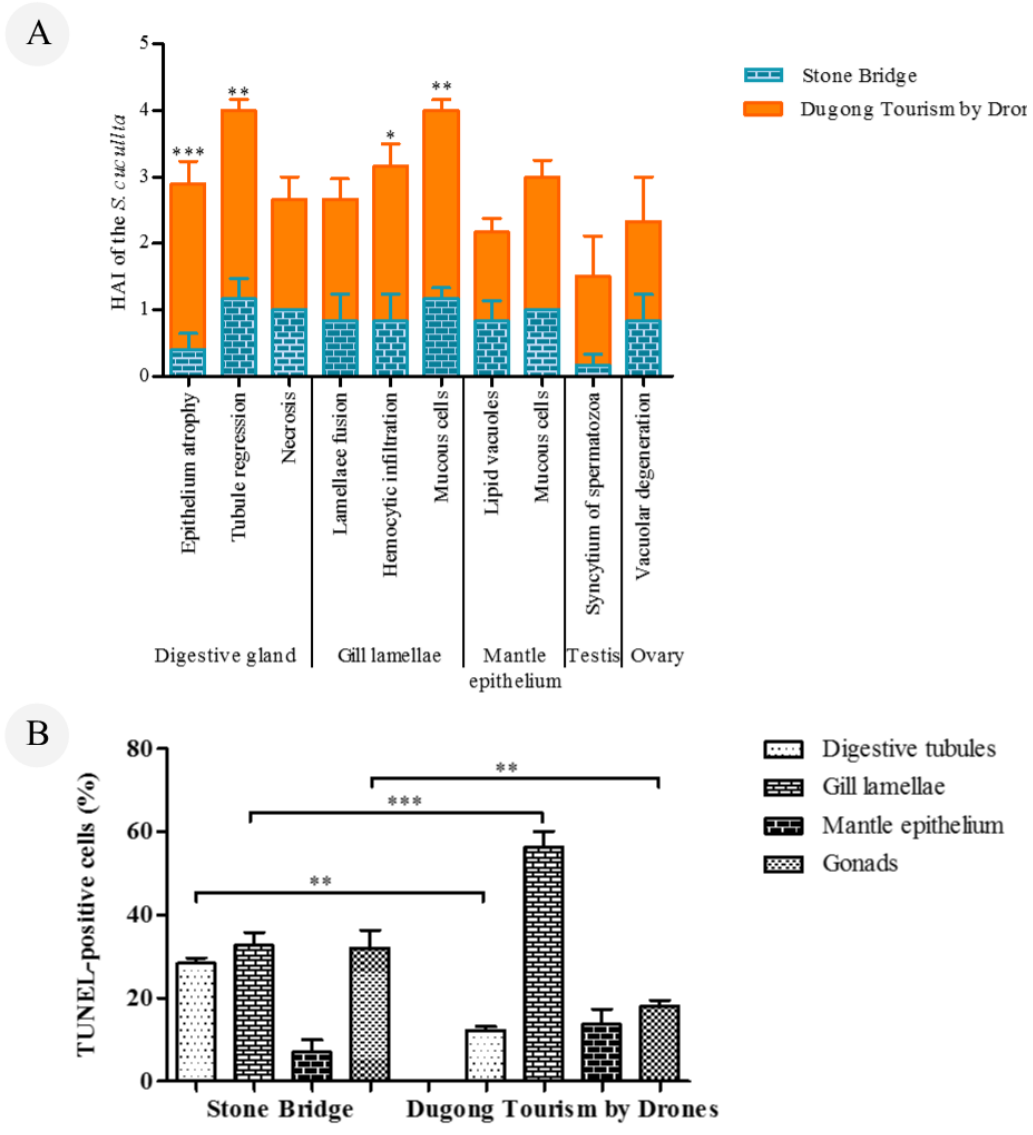


Figure 15 Histopathological assessment of (A) semi-quantitative scoring and (B) The density of apoptotic cells in four tissue of the *S. cucullata* including digestive gland, gill lamellae, mantle epithelium, testis and ovary from between sampling locations. Values are represented as mean \pm SD (n=6). Significant differences between the Stone Bridge site and the Dugong Tourism by Drones site (***) p <0.001; **) p <0.01).

6. Heavy metal accumulations in relation to the density of apoptotic cells

The concentration of four heavy metals including Zn, Pb, Cu, and Cd was measured in the same organs of *S. cucullata* from the two sampling sites (Table 15). In general, Zn, Cu, and Cd levels were higher in samples from the Dugong Tourism by Drones site, whereas Pb showed the opposite tendency. Regarding the organs, the digestive gland generally showed the highest levels of heavy metals except for the Zn concentration in the mantle at the Dugong Tourism by Drones site (706.00 ± 7.99 mg/kg¹ dry weight).

Two-way ANOVA showed that Cd concentration was significantly affected by monitoring sites ($df = 1, F = 1792, p < 0.001$) and organs ($df = 3, F = 55.14, p < 0.01$). Similarly, monitoring sites and organs exerted significant effects on the concentration of Pb ($df = 1, F = 236, p < 0.01$; $df = 3, F = 50.22, p < 0.01$), Cu ($df = 1, F = 1130, p < 0.01$; $df = 3, F = 205.8, p < 0.01$), and Zn ($df = 1, F = 9661, p < 0.01$; $df = 3, F = 1810, p < 0.01$). Most heavy metals concentrations were significantly different between the samples from the two sampling locations in the post-hoc t-test.

Table 15 Mean range and standard deviation of heavy metal toxicity concentration (mg/kg¹ dry weight) in the four tissue of *S. cucullata* from sampling locations

Sites	Organ	Heavy metal concentration (mg/kg ¹ dry weight)			
		Cd	Pb	Cu	Zn
		mean±SD	mean±SD	mean±SD	mean±SD
Stone Bridge	Mantle	2.86±0.38 [*]	16.31±0.93 [*]	112.58±3.04 ^{**}	355.49±3.29 ^{**}
	Gills	1.38±0.22 ^{**}	15.08±1.52	121.89±1.07 ^{**}	256.25±5.60 ^{**}
	Gonad	2.49±0.09 ^{**}	20.99±0.01 [*]	103.01±2.61 [*]	161.16±1.96 [*]
	Digestive gland	5.24±0.26 ^{**}	23.36±0.45 ^{**}	155.95±5.25	534.40±3.07 ^{**}
Dugong Tourism by Drones	Mantle	8.25±0.20	6.48±0.61	188.93±1.82	706.00±7.99
	Gills	9.10±0.50	10.95±2.57	187.02±2.28	580.94±3.94
	Gonad	7.00±0.27	9.31±0.50	135.94±4.87	478.64±9.92
	Digestive gland	9.61±0.18	15.52±0.62	190.52±0.44	638.38±3.96
Standard limitation (mg/kg¹ dry weight)		0.2	2	10	150

Noted: *, ** Significantly different from corresponding values from Dugong Tourism by Drones samples, * $p < 0.05$, ** $p < 0.01$. SD = Standard Deviation, Pb = Lead, Cd = Cadmium, Cu = Copper, Zn = Zinc

Source of the standard limitation: USEPA (2002)

7. Human health risk assessment

The chronic daily intake (CDI) and the hazard quotient (HQ) of *S. cucullata* from the two sampling sites were compared (Table 16). The Dugong Tourism by Drones site showed higher CDI for Cd, Cu, and Zn with the highest value in Zn (0.972 mg/kg per day), whereas the CDI of Pb was higher in the samples from the Stone Bridge site. The HQ values showed the same tendency with the highest value in Cd of *S. cucullata* from the Dugong Tourism by Drones site (13.73), whereas the lowest in Zn recorded in *S. cucullata* from the Stone Bridge site (1.76).

Table 16 The chronic daily intake and the hazard quotient of the heavy metals of the *S. cucullata* specimens between the Stone Bridge site and the Dugong Tourism by Drones site

	Heavy metal parameters	Stone Bridge	Dugong Tourism by Drones	Reference dose
The chronic daily intake (CDI, mg / kg per day).	Pb	0.031	0.016	0.0035
	Cd	0.005	0.014	0.001
	Cu	0.200	0.284	0.04
	Zn	0.529	0.972	0.3
The hazard quotient (HQ)	Pb	8.75	4.67	HQ < 0.1 Represents acceptable level
	Cd	5.24	13.73	0.1 ≥ HQ ≤ 1.0 Low
	Cu	4.99	7.1	1.1 ≥ HQ ≤ 10 Moderate
	Zn	1.76	3.24	HQ > 10 Severe

Note: Pb = Lead, Cd = Cadmium, Cu = Copper, Zn = Zinc

Source of the reference doses: Khan et al. (2008)

CHAPTER V

DISCUSSION AND CONCLUSION

Discussion

Two sampling locations including the Stone Bridge and Dugong Tourism by Drones sites, only water temperature was significantly different in this study. This might be related to the fact that the sampling sites were in the intertidal zone, which is extremely different in water temperatures depending on the season. The temperature is high in summer, and the seasonal effect must be bigger in the shallow areas (Hoa and Wang 2015, Rybovich et al. 2016). We suggest that this difference in water temperature might be responsible for the observed differences in condition factors and reproductive activity of the oysters (Latchere et al. 2018). Indeed, Rajapandian et al. (1990) showed that the water temperature correlated with the CF in *Crassostrea madrasensis* with the highest CF in April. These results were consistent with other previous observations in *Pinctada margaritifera* (Latchere et al. 2018) and *Crassostrea gigas* (Kim and Lozhkin 2021). Additionally, aquatic environment provides the habitat of aquatic animals (Lushchak, 2011; Chandurvelan et al., 2013; Nguyen et al., 2018). The rapid alteration of physical and chemical parameters of the water column hence causes the deterioration of the aquatic animals' s habitats and health (Chapman et al., 1996; Jamdade and Gawande, 2017). In the present study, however, the water parameters were considered to be within the standard range (Howard et al., 2004; Rusydi, 2018), representing the optimum condition for the oyster. The only exception was the water temperature, which was slightly higher than the standard range and was significantly different between the two sites. The high temperature may account for the histopathological alterations observed in this study, although the heavy metals are more likely to be responsible because their concentrations were far above the standard limitation. It would be useful in future studies to have the seasonal sampling to accurately examine the effect of water temperature on the oyster

It was clear from the morphometric characteristics that *S. cucullata* from the Stone Bridge area was smaller than those from Dugong Tourism by Drones. Since the

tested parameters such as CF are closely related to the available food in oysters (Pouvreau et al. 2000, Lim et al. 2020), Dugong Tourism by Drones might represent a favorable environment for *S. cucullata* compared to Stone Bridge. The high growth and CF have been associated with the feeding activity in *Hemifusus ternatanus* under artificial conditions (Yang et al. 2020) and *Pinctada margaritifera var erythraensis* collected from Dongonab Bay, Red Sea, Sudan (Elamin and Eldin 2015).

The structure of digestive gland, gills, gonads and mantle of *S. cucullata* was similar to those in other bivalves including *Pecten maximus*, *Mytilus edulis*, and *Crassostrea gigas* (Beninger et al. 1994, Cannuel et al. 2009, Dutertre et al. 2017). Interestingly, the length of gill lamellae and mantle of this oyster showed significant differences between the two sampling locations. This might be related to the different rate of development since these organs are involved in respiration and feeding (Zhang et al. 2021). It was reported in Cannuel and Beninger (2006), gill development in *Crassostrea gigas* juveniles was a rapid development to increase food-feeding efficiency.

This study also showed that *S. cucullata* has the protandric characteristics with no statistically significant differences in the gonadal development between the two locations. The male gonad began to develop in the 1-2 cm size group, whereas the female gonad did in the 2.1-3 cm size group, which corresponds to the juvenile stage. This indicated the current oysters start life as male and changed permanently into female after about a year or increased size. Similar gonadal maturation patterns were found in other bivalves including *Crassostrea glomerata* (Dinamani 1974), *Crassostrea corteziensis* (Rodríguez-Jaramillo et al. 2008), *Haliotis discus hannai* (Awaji and Hamano 2004). The beginning of the adult stage was considered to be adult at 4.1-5 cm similar to other bivalves such as *Crassostrea gigas* (Mizuta et al. 2012) and *Crassostrea iredalei* (Chueachat et al. 2018).

The Msc of *S. cucullata* had oval, cup-shaped, and pear-shaped, which is similar to the findings in *Haliotis diversicolor* (Di et al. 2012), *Solen grandis Dunker* (Xiuzhen et al. 2003), *Chaetopleura angulata* and *Acanthochitona fascicularis* (Lobo-Da-Cunha et al. 2022). Msc is essential to marine mollusks in producing various functional substances together with glands in the epithelium that procedure exudate. The highest densities of Msc was observed in the digestive gland, suggesting that it is the main

organ for mucus production. This was similar to the findings of Yonge (1926), and the mucus in the digestive organs has various roles including food locomotion and the immune activity (Allam et al. 2013). The maximum density of *S. cucullata* Msc was observed in the 3.1-4 cm size group, and dramatic decrease in Msc was observed in the 4.1-5 cm size groups. This might be related to the environmental situation, but requires further investigations.

Gills exert multiple functions including the respiration, osmoregulation, and excretion through the direct contact with the external environment (Khan et al., 2018; Da Silva et al., 2006). This organ is considered as the main target of contaminants (Khan et al., 2018; Da Silva et al., 2006; Chandurvelan et al., 2013) as similarly observed in our data. Integrated biomarkers of histopathology, apoptosis, and HAI valve consistently showed the highest damage in the gill lamellae of *S. cucullata* compared to other organs, especially in samples from the Dugong Tourism by Drones site. These findings are in accordance with observation in the Pacific oyster *Magallana gigas* with the occurrence of gill histological alterations (Otegui et al., 2023). Al-Hashem (2017) similarly found the gill abnormality including the complete degeneration of gill filaments of the pearl oyster, *Pinctada radiata*, after exposure to the toxic pollutants from the coast of Kuwait, which is also in agreement with Cengiz (2006). These results indicate that the oysters from the Dugong Tourism by Drones site may be strongly impacted by the environmental stressors. Since the necrotic and degenerative alterations of gill lamellae can disturb its respiratory and osmoregulatory functions (Cengiz, 2006), *S. cucullata* in Libong Island may also experience oxygen deficiency as reported in previous observations (Abdel-Moneim et al., 2018; Otegui et al. 2023).

Bivalves are capable of accumulating environmental heavy metals in their tissues (Mok et al., 2015; De Mora et al., 20), which was similarly observed in *S. cucullata* in the present study. Concentrations of the four selected heavy metals including Zn, Pb, Cu, and Cd were mostly higher in *S. cucullata* from the Dugong Tourism by Drones site. Similarly, Kobkeatthawin et al. (2021) reported that Fe, Cu, Co, Pb, Mn, and Ni were accumulated in the soft tissue of *Strombus canarium* from Libong Island. Very little is known about the original sources of these heavy metals in Libong Island, but previous investigators suggested the relation to anthropogenic

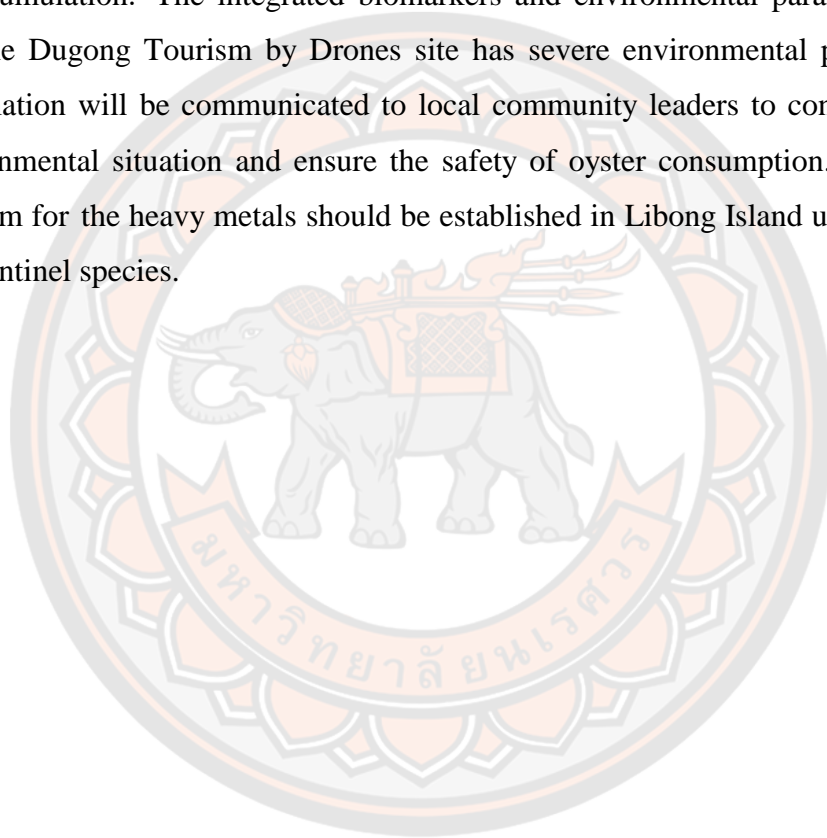
activities and agriculture (Kobkeatthawin et al., 2021) from the observation of many marine wastes, microplastics, and batteries from the communities (Pradit et al., 2020).

The concentrations of heavy metals, especially those of Cu and Zn in the digestive gland and gill of *S. cucullata*, were significantly differed between the sites with high values in the Dugong Tourism by Drones site. The association between the heavy metal concentrations and integrative biomarkers suggests the causal role of these heavy metals in the observed alterations, although the used biomarkers can also be observed in tissues under normal conditions (Bryan, 1971; Barile, 2008), especially in the sensitive organs such as the digestive gland and gill (Lu-Yan et al., 2021; Pakingking et al., 2022; Rodney et al., 2007; Pham, 2020; Luo et al., 2014; Samsi and Karim, 2019). Osuna-Martínez et al. (2011) and Ochoa et al. (2013) reported the high accumulation of heavy metals in the digestive gland of oyster.

The heavy metal levels determined in this study all exceeded the maximum ranges according to standards limitation (USEPA, 2002) together with the chronic daily intake (CDI) and the hazard quotient (HQ) to assess the Human Health Risk Assessment (HHRI). Especially $HQ > 0.1$ indicates the hazard to human consumption that may cause a serious problem for the health of people feeding on the oyster. This is the first report of heavy metal concentrations and risk assessment of *S. cucullata* from the Libong Island, which should be immediately disseminated. However, the limitation of this study was controlled by the sample size collected from sampling locations. Therefore, the study required a large sample for investigation. Accumulation of heavy metals in human should also be investigated in further studies.

Conclusion

The histological observations of *S. cucullata* from Libong Island identified their juvenile (<4 cm) and adult (>4 cm) stages with the size of their organs, including the digestive gland, gills, and mantle. The present observation also revealed the size at sexual maturation, at which gametogenesis begins, although it is influenced by environmental conditions and nutrients. An identified histopathological alterations and apoptotic cells in *S. cucullata*, which could be related to the heavy metal bioaccumulation. The integrated biomarkers and environmental parameters showed that the Dugong Tourism by Drones site has severe environmental problems. This information will be communicated to local community leaders to concern about the environmental situation and ensure the safety of oyster consumption. A monitoring program for the heavy metals should be established in Libong Island using this oyster as a sentinel species.



REFERENCES



REFERENCES

- Abdel-Moneim, A. M., Alkahtani, M. A., Elmenshawy, O. M., Elsayy, H., Hafez, A. M., & Genena, M. (2018). Monitoring metal levels in water and multiple biomarkers in the grouper (*Epinephelus tauvina*) to assess environmental stressors on the Arabian Gulf coast of Saudi Arabia. *Toxicology and Industrial Health*, *34*(5), 301–314. <https://doi.org/10.1177/0748233718754980>
- Adams, D. H., Sonne, C., Basu, N., Dietz, R., Nam, D. H., Leifsson, P. S., & Jensen, A. L. (2010). Mercury contamination in spotted seatrout, *Cynoscion nebulosus*: An assessment of liver, kidney, blood, and nervous system health. *Science of the Total Environment*, *408*(23), 5808–5816. <https://doi.org/10.1016/j.scitotenv.2010.08.019>
- Adeyemi, J. A., & Deaton, L. E. (2012). The effect of cadmium exposure on digestive enzymes in the Eastern oyster *Crassostrea virginica*. *Journal of Shellfish Research*, *31*(3), 631–634. <https://doi.org/10.2983/035.031.0306>
- Aguirre-Rubí, J. R., Luna-Acosta, A., Ortiz-Zarragoitia, M., Zaldibar, B., Izagirre, U., Ahrens, M. J., Marigómez, I. (2018). Assessment of ecosystem health disturbance in mangrove-lined Caribbean coastal systems using the oyster *Crassostrea rhizophorae* as sentinel species. *Science of the Total Environment*, *618*, 718–735. <https://doi.org/10.1016/j.scitotenv.2017.08.098>
- Al-Hashem, M. A. (2017). Gill histopathological effects of PAHs on adult pearl oyster, *Pinctada radiata*; at Al-Khiran Coast in Kuwait. *Journal of Environmental Protection*, *08*(02), 109–119. <https://doi.org/10.4236/jep.2017.82009>
- Allam, B., Carden, W. E., Ward, J. E., Ralph, G. M., Winnicki, S., & Espinosa, E. P. (2013). Early host-pathogen interactions in marine bivalves: Evidence that the alveolate parasite *Perkinsus marinus* infects through the oyster mantle during rejection of pseudofeces. *Journal of Invertebrate Pathology*, *113*(1), 26–34. <https://doi.org/10.1016/j.jip.2012.12.011>
- Amadi, C. N., Frazzoli, C., & Orisakwe, O. E. (2020). Sentinel species for biomonitoring and biosurveillance of environmental heavy metals in Nigeria. *Journal of Environmental Science and Health, Part A*, *38*(1), 21–60. <https://doi.org/10.1080/26896583.2020.1714370>

- AOAC (2005) Official method of analysis. 18th edition, Association of Officiating Analytical Chemists, Washington DC, Method 935.14 and 992.24.
- Awaji, M., & Hamano, K. (2004). Gonad formation, sex differentiation and gonad maturation processes in artificially produced juveniles of the abalone, *Haliotis discus hannai*. *Aquaculture*, 239(1–4), 397–411. <https://doi.org/10.1016/j.aquaculture.2004.03.010>
- Baralla, E., Pasciu, V., Varoni, M. V., Nieddu, M., Demuro, R., & Demontis, M. P. (2021). Bisphenols' occurrence in bivalves as sentinel of environmental contamination. *Science of the Total Environment*, 785, 147263. <https://doi.org/10.1016/j.scitotenv.2021.147263>
- Barile, F. A. (2007). Principles of toxicology testing. *CRC Press eBooks*. <https://doi.org/10.1201/9781420008326>
- Bekiari, A. and Manoli, P. (2016). EFL teacher verbal aggressiveness and argumentativeness and student Socio-Affective Strategy use and affective learning exploring possible associations. *Journal of Teacher Education and Educators*, 5, 154-171.
- Beninger, P. G., Dwiono, S. A. P., & Penneç, M. L. (1994). Early development of the gill and implications for feeding in *Pecten maximus* (Bivalvia: Pectinidae). *Marine Biology*, 119(3), 405–412. <https://doi.org/10.1007/bf00347537>
- Bryan G.W. (1971). The effects of heavy metals (other than mercury) on marine and estuarine organisms. *Proceedings of the Royal Society of London*, 177(1048), 389–410. <https://doi.org/10.1098/rspb.1971.0037>
- Bryan, G. W., Gibbs, P., Hummerstone, L. G., & Burt, G. R. (1986). The Decline of the Gastropod *Nucella Lapillus* around South-West England: Evidence for the effect of tributyltin from antifouling paints. *Journal of the Marine Biological Association of the United Kingdom*, 66(3), 611–640. <https://doi.org/10.1017/s0025315400042247>
- Cannuel, R., & Beninger, P. G. (2006). Gill development, functional and evolutionary implications in the Pacific oyster *Crassostrea gigas* (Bivalvia: Ostreidae). *Marine Biology*, 149(3), 547–563. <https://doi.org/10.1007/s00227-005-0228-6>
- Cannuel, R., Beninger, P. G., McCombie, H., & Boudry, P. (2009). Gill development and its functional and evolutionary implications in the Blue Mussel *Mytilus*

- edulis* (Bivalvia: Mytilidae). *The Biological Bulletin*, 217(2), 173–188.
<https://doi.org/10.1086/bblv217n2p173>
- Cardoso, I. D. S., Alves, E. V. B., Rodrigues, L. L., Guedes, A., De Oliveira, L. C., De Quadros, M. L. A., Da Silva, F. N. L. (2021). Can the *Ucides Cordatus* fishing and the *Crassostrea Gasar* creation on the Amazon coast make up the curriculum of rural schools. *Journal of Fisheries Science*, 3(1).
<https://doi.org/10.30564/jfsr.v3i1.3290>
- Castilho-Westphal, G. G., Magnani, F. P., & Ostrensky, A. (2013). Gonad morphology and reproductive cycle of the mangrove oyster *Crassostrea brasiliiana* (Lamarck, 1819) in the baía de Guaratuba, Paraná, Brazil. *Acta Zoologica*, 96(1), 99–107. <https://doi.org/10.1111/azo.12055>
- Cengiz, E. İ. (2006). Gill and kidney histopathology in the freshwater fish *Cyprinus carpio* after acute exposure to deltamethrin. *Environmental Toxicology and Pharmacology*, 22(2), 200–204. <https://doi.org/10.1016/j.etap.2006.03.006>
- Ceylan, Ş., & Kaptaner, B. (2019). Apoptosis and cell proliferation in the epithelia of the esophagus and intestine of *Alburnus tarichi* Gldenstdt, 1814 (Cyprinidae) during migration from highly alkaline and brackish water to fresh water. *The European Zoological Journal*, 86(1), 103–112.
<https://doi.org/10.1080/24750263.2019.1604833>
- Chapman, P.M., Allen, H.E., Godtfredsen, K., Z'Graggen, M.N., (1996). Policy analysis, peer reviewed: evaluation of bioaccumulation factors in regulating metals. *Journal of Environmental Science and Technology*, 30 (10), 448–452.
<https://doi.org/10.1021/es962436d>
- Chandurvelan, R., Marsden, I. D., Gaw, S., & Glover, C. N. (2013). Waterborne cadmium impacts immunocytotoxic and cytogenotoxic endpoints in green-lipped mussel, *Perna canaliculus*. *Aquatic Toxicology*, 142–143, 283–293.
<https://doi.org/10.1016/j.aquatox.2013.09.002>
- Cheng, T. C., & Sullivan, J. T. (1984). Effects of heavy metals on phagocytosis by molluscan hemocytes. *Marine Environmental Research*, 14(1–4), 305–315.
[https://doi.org/10.1016/0141-1136\(84\)90084-9](https://doi.org/10.1016/0141-1136(84)90084-9)

- Chiarelli, R., & Roccheri, M. C. (2014). Marine invertebrates as bioindicators of heavy metal pollution. *Open Journal of Metal*, 04(04), 93–106. <https://doi.org/10.4236/ojmetal.2014.44011>
- Chueachat, P., Tarangkoon, W., & Tanyaros, S. (2018). A comparative study on the nursery culture of hatchery-reared sub-adult cupped oyster, *Crassostrea iredalei* (Faustino, 1932), in an earthen pond and a mangrove canal. *Fisheries & Aquatic Life*, 26(4), 217–222. <https://doi.org/10.2478/aopf-2018-0024>
- Da Silva, P. M., Villalba, A., & Sunila, I. (2006). Branchial lesions associated with abundant apoptotic cells in oysters *Ostrea edulis* of Galicia (NW Spain). *Diseases of Aquatic Organisms*, 70, 129–137. <https://doi.org/10.3354/dao070129>
- De Mora, S., Fowler, S. W., Wyse, E., & Azemard, S. (2004). Distribution of heavy metals in marine bivalves, fish and coastal sediments in the Gulf and Gulf of Oman. *Marine Pollution Bulletin*, 49(5–6), 410–424. <https://doi.org/10.1016/j.marpolbul.2004.02.029>
- Denil, D. J., Ching, F. F., & Ransangan, J. (2017). Health risk assessment due to heavy metals exposure via consumption of bivalves harvested from Marudu Bay, Malaysia. *Open Journal of Marine Science*, 07(04), 494–510. <https://doi.org/10.4236/ojms.2017.74035>
- Dennis, M. M., Diggles, B. K., Faulder, R., Olyott, L. J. H., Pyecroft, S., Gilbert, G., & Landos, M. (2016). Pathology of finfish and mud crabs *Scylla serrata* during a mortality event associated with a harbour development project in Port Curtis, Australia. *Diseases of Aquatic Organisms*, 121(3), 173–188. <https://doi.org/10.3354/dao03011>
- Di, G., Ni, J., Zhang, Z., Wang, Y., Wang, B., & Ke, C. (2012). Types and distribution of mucous cells of the abalone *Haliotis diversicolor*. *African Journal of Biotechnology*, 11(37). <https://doi.org/10.5897/ajb10.2066>
- Dutertre, M., Ernande, B., Haure, J., & Barillé, L. (2016). Spatial and temporal adjustments in gill and palp size in the oyster *Crassostrea gigas*. *Journal of Molluscan Studies*, 83(1), 11–18. <https://doi.org/10.1093/mollus/eyw025>
- Elamin, M., & Eldin, M.E. (2015). Productivity and economic values of the pearl oyster (*Pinctada margaritifera var erythraensis*) cultured in Dongonab Bay, Red Sea.

International Journal of Environmental Science and Technology, 1(7):1193 – 1204.

- Fang, Z., Cheung, R., & Wong, M. H. (2001). Heavy metal concentrations in edible bivalves and gastropods available in major markets of the Pearl River Delta. *PubMed*, 13(2), 210–217. Retrieved from <https://pubmed.ncbi.nlm.nih.gov/11590745>
- Ferreira-Cravo, M., Ventura-Lima, J., Sandrini, J. Z., Amado, L. L., Geracitano, L. A., De Freitas Rebelo, M., Monserrat, J. M. (2009). Antioxidant responses in different body regions of the polychaeta *Laeonereis acuta* (Nereididae) exposed to copper. *Ecotoxicology and Environmental Safety*, 72(2), 388–393. <https://doi.org/10.1016/j.ecoenv.2008.07.003>
- Fukunaga, A., & Anderson, M. J. (2011). Bioaccumulation of copper, lead and zinc by the bivalves *Macomona liliana* and *Austrovenus stutchburyi*. *Journal of Experimental Marine Biology and Ecology*, 396(2), 244–252. <https://doi.org/10.1016/j.jembe.2010.10.029>
- Galaris, D., & Evangelou, A. (2002). The role of oxidative stress in mechanisms of metal-induced carcinogenesis. *Critical Reviews in Oncology/Hematology*, 42(1), 93–103. [https://doi.org/10.1016/s1040-8428\(01\)00212-8](https://doi.org/10.1016/s1040-8428(01)00212-8)
- Galasso, C., D’Aniello, S., Sansone, C., Ianora, A., & Romano, G. (2019). Identification of cell death genes in sea urchin *Paracentrotus lividus* and their expression patterns during embryonic development. *Genome Biology and Evolution*, 11(2), 586–596. <https://doi.org/10.1093/gbe/evz020>
- García-Corona, J. L., Rodríguez-Jaramillo, C., Saucedo, P. E., López-Carvallo, J. A., Arcos-Ortega, G. F., & Mazón-Suástegui, J. M. (2018). Internal energy management associated with seasonal gonad development and oocyte quality in the horse mussel *Modiolus capax* (Bivalvia; Mytilidae). *Journal of Shellfish Research*, 37(3), 475–483. <https://doi.org/10.2983/035.037.0302>
- Guzmán-García, X., Botello, A. V., Martínez-Tabche, L., & González-Márquez, H. (2008). Effects of heavy metals on the oyster (*Crassostrea virginica*) at Mandinga Lagoon, Veracruz, Mexico. *Revista De Biología Tropical*, 57(4). <https://doi.org/10.15517/rbt.v57i4.5439>

- He, Y., Fang, H., Pan, X., Zhu, B., Chen, J., Wang, J., & Zhang, H. (2023). Cadmium exposure in aquatic products and health risk classification assessment in residents of Zhejiang, China. *Foods*, 12(16), 3094. <https://doi.org/10.3390/foods12163094>
- Hietanen, C., Sunila, I., & Kristoffersson, R.. (1988). Toxic effects of zinc on the common mussel *mytilus edulis* l. bivalvia in brackish water. physiological and histopathological studies. *Annales Zoologici Fennici*, 25(4), 341–347.
- Hoa, H. T., & Wang, C. L. (2015). The effects of temperature and nutritional conditions on *Mycelium* growth of two oyster mushrooms (*Pleurotus ostreatus* and *Pleurotus cystidiosus*). *Mycobiology*, 43(1), 14–23. <https://doi.org/10.5941/myco.2015.43.1.14>
- Hong, T.K., Bobby, G., Siti N., Addis, K., Musa, N., Mohd, E., Wahid, A. and Zainathan, S.C. (2017). Histopathology conditions of cultured oyster, *Crassostrea iredalei* from southern and east Malaysia. *AAAL Bioflux*, 10(2), 445 – 454.
- Howard, D.W., Keller, B.J., Lewis, E.J., Smith, C.S. (2004). Histological techniques for marine bivalve mollusks and crustaceans. Amsterdam, The Netherlands, pp 59-79.
- Jahan, S., & Strezov, V. (2019). Assessment of trace elements pollution in the sea ports of New South Wales (NSW), Australia using oysters as bioindicators. *Scientific Reports*, 9(1). <https://doi.org/10.1038/s41598-018-38196-w>
- Jamdade, A. B., & Gawande, S. M., (2017). Analysis of water quality parameters: a review. *International Journal of Engineering Research*. 6 (3), 145–148.
- Khan, M., Masroor, R., Khan, A., Gulfam, N., Siraj, M., Zaidi, F., & Qadir, F. (2018). Bioaccumulation of heavy metals in water, sediments, and tissues and their histopathological effects on *Anodonta cygnea* (Linea, 1876) in Kabul River, Khyber Pakhtunkhwa, Pakistan. *BioMed Research International*, 2018, 1–10. <https://doi.org/10.1155/2018/1910274>
- Kim, A. C. & Lozhkin, D. M. (2021). “Influence of total water-temperature value on the size and weight characteristics of Pacific oyster *Crassostrea gigas* (Thunberg, 1793) in the Aniva Bay (Sakhalin Island) according to Satellite

- Data.” *Izvestiya Atmospheric and Oceanic Physics* 57(12):1712–19. [https://doi: 10.1134/s0001433821120124](https://doi.org/10.1134/s0001433821120124).
- Kobkeatthawin, T., Sirivithayapakorn, S., Nitiratsuwan, T., Muenhor, D., Loh, P. S., & Pradit, S. (2021). Accumulation of trace metal in sediment and soft tissue of *Strombus canarium* in a tropical remote Island of Thailand. *Journal of Marine Science and Engineering*, 9(9), 991. <https://doi.org/10.3390/jmse9090991>
- Kong, N., Zhao, Q., Liu, C., Li, J., Liu, Z., Gao, L., Song, L. (2020). The involvement of zinc transporters in the zinc accumulation in the Pacific oyster *Crassostrea gigas*. *Gene*, 750, 144759. <https://doi.org/10.1016/j.gene.2020.144759>
- Kongthong, K., Charoenphon, N., Thaochan, N., Boonyoung, P., Lida, A., Jeamah, A., Senarat, S. (2022). A histological method for marine invertebrates. *Veterinary Integrative Sciences*, 21(1), 251–263. <https://doi.org/10.12982/vis.2023.020>
- Kongthong, K., Senarat S., Inchan A., Kaneko G, Lda A, Phoungpetchara P, Charoenphon N. 2023. “Size distribution and organ development of the hooded oyster, *Saccostrea cucullata* (Born, 1778) from Libong Island, Thailand.” *ScienceAsia*.
- Landos, M., Smith, M. L., & Immig, J. (2021). Aquatic pollutants in oceans and fisheries | IPEN. Retrieved from <https://policycommons.net/artifacts/1526456/aquatic-pollutants-in-oceans-and-fisheries-ipen/2214687/>
- Lasi, M., David, C. N., & Böttger, A. (2009). Apoptosis in pre-Bilaterians: Hydra as a model. *Apoptosis*, 15(3), 269–278. <https://doi.org/10.1007/s10495-009-0442-7>
- Latchere, O., Mehn, V., Gaertner-Mazouni, N., Moullac, G. L., Fiévet, J., Belliard, C., Saulnier, D. (2018). Influence of water temperature and food on the last stages of cultured pearl mineralization from the black-lip pearl oyster *Pinctada margaritifera*. *PLOS ONE*, 13(3), e0193863. <https://doi.org/10.1371/journal.pone.0193863>
- Li, X. F., Wang, P. F., Feng, C., Liu, D. Q., Chen, J. K., & Wu, F. (2018). Acute toxicity and hazardous concentrations of zinc to native freshwater organisms under different pH values in China. *Bulletin of Environmental Contamination and Toxicology*, 103(1), 120–126. <https://doi.org/10.1007/s00128-018-2441-2>

- Lim, L., Liew, K., Yap, T., Tan, N., & Shi, C. (2020). Length-weight relationship and relative condition factor of pearl oyster, *Pinctada fucata martensii*, cultured in the Tieshangang Bay of the Beibu Gulf, Guangxi Province, China. *Borneo Journal of Marine Science and Aquaculture (BJoMSA)*, 4(1), 24–27. <https://doi.org/10.51200/bjomsa.v4i1.2048>
- Lionetto, M. G., Caricato, R., & Giordano, M. E. (2019). Pollution biomarkers in environmental and human biomonitoring. *The Open Biomarkers Journal*, 9(1), 1–9. <https://doi.org/10.2174/1875318301909010001>
- Lobo-da-Cunha, A., Alves, Â., Oliveira, E., & Calado, G. (2022). Functional histology and ultrastructure of the digestive tract in two species of chitons (Mollusca, Polyplacophora). *Journal of Marine Science and Engineering*, 10(2), 160. <https://doi.org/10.3390/jmse10020160>
- Lu, G., Ke, C., Zhu, A., & Wang, W. (2017). Oyster-based national mapping of trace metals pollution in the Chinese coastal waters. *Environmental Pollution*, 224, 658–669. <https://doi.org/10.1016/j.envpol.2017.02.049>
- Luo, L., Ke, C., Guo, X., Shi, B., & Huang, M. (2014). Metal accumulation and differentially expressed proteins in gill of oyster (*Crassostrea hongkongensis*) exposed to long-term heavy metal-contaminated estuary. *Fish & Shellfish Immunology*, 38(2), 318–329. <https://doi.org/10.1016/j.fsi.2014.03.029>
- Lushchak, V. I. (2011). Environmentally induced oxidative stress in aquatic animals. *Aquatic Toxicology*, 101(1), 13–30. <https://doi.org/10.1016/j.aquatox.2010.10.006>
- Lu-Yan, Q., Zhang, R., Liang, Y., Wu, L., Zhang, Y., Mu, Z., Yu, Z. (2021). Concentrations and health risks of heavy metals in five major marketed marine bivalves from three coastal cities in Guangxi, China. *Ecotoxicology and Environmental Safety*, 223, 112562. <https://doi.org/10.1016/j.ecoenv.2021.112562>
- Mesquita, A. F., Marques, S. M., Marques, J. C., Gonçalves, F., & Gonçalves, A. M. (2019). Copper sulphate impact on the antioxidant defence system of the marine bivalves *Cerastoderma edule* and *Scrobicularia plana*. *Scientific Reports*, 9(1). <https://doi.org/10.1038/s41598-019-52925-9>

- Mizuta, D. D., Júnior, N. S., Fischer, C., & Lemos, D. (2012). Interannual variation in commercial oyster (*Crassostrea gigas*) farming in the sea (Florianópolis, Brazil, 27°44' S; 48°33' W) in relation to temperature, chlorophyll a and associated oceanographic conditions. *Aquaculture*, 366–367, 105–114. <https://doi.org/10.1016/j.aquaculture.2012.09.011>
- Mok, J. S., Yoo, H. D., Kim, P. H., Yoon, H. D., Park, Y. C., Lee, T. S., Kim, J. H. (2015). Bioaccumulation of Heavy Metals in Oysters from the Southern Coast of Korea: Assessment of Potential Risk to Human Health. *Bulletin of Environmental Contamination and Toxicology*, 94(6), 749–755. <https://doi.org/10.1007/s00128-015-1534-4>
- National Research Council (US) Committee on Animals as Monitors of Environmental Hazards. *Animals as Sentinels of Environmental Health Hazards*. Washington (DC): National Academies Press (US); 1991. Available from: <https://www.ncbi.nlm.nih.gov/books/NBK234944/> doi: 10.17226/1351
- Nguyen, T. V., Alfaro, A. C., Mérien, F., Lulijwa, R., & Young, T. (2018). Copper-induced immunomodulation in mussel (*Perna canaliculus*) haemocytes. *Metallomics*, 10(7), 965–978. <https://doi.org/10.1039/c8mt00092a>
- Nishijo, M., Nakagawa, H., Suwazono, Y., Nogawa, K., & Kido, T. (2017). Causes of death in patients with Itai-itai disease suffering from severe chronic cadmium poisoning: a nested case–control analysis of a follow-up study in Japan. *BMJ Open*, 7(7), e015694. <https://doi.org/10.1136/bmjopen-2016-015694>
- Ochoa, V., Barata, C., & Riva, M. C. (2013). Heavy metal content in oysters (*Crassostrea gigas*) cultured in the Ebro Delta in Catalonia, Spain. *Environmental Monitoring and Assessment*, 185(8), 6783–6792. <https://doi.org/10.1007/s10661-013-3064-z>
- OIE. (2021). *Diseases of mollusc manual of diagnostic tests for aquatic animals*. OIE representation for Asia and the Pacific. Tokyo, Japan. pp 1-414.
- Os, O. (2017). Physiological, immunological, genotoxic and histopathological biomarker responses of molluscs to heavy metal and water-quality parameter exposures: A critical review. *Journal of Oceanography and Marine Research*, 05(01). <https://doi.org/10.4172/2572-3103.1000158>

- Osuna-Martínez, C. C., Páez-Osuna, F., & Alonso-Rodríguez, R. (2011). Cadmium, copper, lead and zinc in cultured oysters under two contrasting climatic conditions in coastal lagoons from SE Gulf of California, Mexico. *Bulletin of Environmental Contamination and Toxicology*, 87(3), 272–275. <https://doi.org/10.1007/s00128-011-0355-3>
- Otegui, M. B. P., Fiori, S., Menechella, A. G., Santos, E. P. D., & Giménez, J. (2023). Histological characterization and morphological alterations in gill and digestive gland in non-native bivalve from the Province of Buenos Aires: spatial and seasonal evaluation. *Research Square (Research Square)*. <https://doi.org/10.21203/rs.3.rs-3126138/v1>
- Pakingking, R. V., Hualde, M. L., Peralta, E. M., Faisan, J. P., & Usero, R. C. (2022). Microbiological quality and heavy metal concentrations in slipper oyster (*Crassostrea iredalei*) cultured in major growing areas in Capiz Province, Western Visayas, Philippines: Compliance with international shellfish safety and sanitation standards. *Journal of Food Protection*, 85(1), 13–21. <https://doi.org/10.4315/jfp-21-257>
- Pascal, P., Fleeger, J. W., Gálvez, F., & Carman, K. R. (2010). The toxicological interaction between ocean acidity and metals in coastal meiobenthic copepods. *Marine Pollution Bulletin*, 60(12), 2201–2208. <https://doi.org/10.1016/j.marpolbul.2010.08.018>
- Pham, T. (2020). Accumulation, depuration and risk assessment of cadmium (Cd) and lead (Pb) in clam *Corbicula fluminea* (O. F. Müller, 1774) under laboratory conditions. *Iranian Journal of Fisheries Sciences*, 19(3), 1062–1072. <https://doi.org/10.22092/ijfs.2018.116877>
- Pouvreau, S., Tiapari, J., Gangnery, A., Lagarde, F., Garnier, M., Teissier, H., & Bodoy, A. (2000). Growth of the black-lip pearl oyster, *Pinctada margaritifera*, in suspended culture under hydrobiological conditions of Takapoto lagoon (French Polynesia). *Aquaculture*, 184(1–2), 133–154. [https://doi.org/10.1016/s0044-8486\(99\)00319-1](https://doi.org/10.1016/s0044-8486(99)00319-1)
- Pradit, S., Towatana, P., Nitiratsuan, T., Jualaong, S., Jirajarus, M., Sornplang, K., & Weerawong, C. (2020). Occurrence of microplastics on beach sediment at

- Libong, a pristine island in Andaman Sea, Thailand. *Scienceasia*, 46(3), 336. <https://doi.org/10.2306/scienceasia1513-1874.2020.042>
- Rajapandian, M. E., Gopinathan, C. P., Rodrigo, J. X., & Gandhi, A. D. (1990). Environmental characteristics of edible oyster beds in and around Tuticorin. *J Mar Biol Assoc India*. Retrieved from <http://eprints.cmfri.org.in/1106/>
- Ramadhaniaty, M., Setyobudiandi, I., & Madduppa, H. (2018). Morphogenetic and population structure of two species marine bivalve (Ostreidae: *Saccostrea cucullata* and *Crassostrea iredalei*) in Aceh, Indonesia. *Biodiversitas*. <https://doi.org/10.13057/biodiv/d190329>
- Rodney, E., Herrera, P., Luxama, J. D., Boykin, M., Crawford, A., Carroll, M., & Catapane, E. J. (2007). Bioaccumulation and tissue distribution of arsenic, cadmium, copper and zinc in *Crassostrea virginica* grown at two different depths in Jamaica Bay, New York. *PubMed*. Retrieved from <https://pubmed.ncbi.nlm.nih.gov/21841973>
- Rodríguez-Jaramillo, C., Hurtado, M., Romero-Vivas, E., Ramírez, J. L., Manzano, M., & Palacios, E. (2008). Gonadal development and histochemistry of the Tropical oyster, *Crassostrea corteziensis* (Hertlein, 1951) during an Annual Reproductive Cycle. *Journal of Shellfish Research*, 27(5), 1129–1141. <https://doi.org/10.2983/0730-8000-27.5.1129>
- Rusydi, A. F. (2018). Correlation between conductivity and total dissolved solid in various type of water: A review. *IOP Conference Series*, 118, 012019. <https://doi.org/10.1088/1755-1315/118/1/012019>
- Rybovich, M., La Peyre, M. K., Hall, S. G., & La Peyre, J. F. (2016). Increased temperatures combined with lowered salinities differentially impact oyster size class growth and mortality. *Journal of Shellfish Research*, 35(1), 101–113. <https://doi.org/10.2983/035.035.0112>
- Samsi, A. N., & Karim, S. A. (2019). The relationship between the length and weight of snail *Nerita lineata* Gmelin 1791 on environmental factors in the mangrove ecosystem. *Journal of Physics*, 1341, 022022. <https://doi.org/10.1088/1742-6596/1341/2/022022>

- Santhanam, R. (2018). Biology and ecology of edible marine bivalve molluscs. In *Apple Academic Press eBooks* (pp. 11–18). <https://doi.org/10.1201/9781315111537-2>
- Sithole, S. C., Agboola, O. O., Mugivhisa, L. L., Amoo, S. O., & Olowoyo, J. O. (2022). Elemental concentration of heavy metals in oyster mushrooms grown on mine polluted soils in Pretoria, South Africa. *Journal of King Saud University - Science*, *34*(2), 101763. <https://doi.org/10.1016/j.jksus.2021.101763>
- Stankovic, M., Hayashizaki, K., Tuntiprapas, P., Rattanachot, E., & Prathep, A. (2021). Two decades of seagrass area change: Organic carbon sources and stock. *Marine Pollution Bulletin*, *163*, 111913. <https://doi.org/10.1016/j.marpolbul.2020.111913>
- Sun, M., Liu, G., Lin, H., Zhang, T., & Guo, W. (2018). Effect of salinity on the bioaccumulation and depuration of cadmium in the pacific cupped oyster, *Crassostrea gigas*. *Environmental Toxicology and Pharmacology*, *62*, 88–97. <https://doi.org/10.1016/j.etap.2018.05.018>
- Sunila, I., & Labanca, J. (2003). Apoptosis in the pathogenesis of infectious diseases of the eastern oyster *Crassostrea virginica*. *Diseases of Aquatic Organisms*, *56*, 163–170. <https://doi.org/10.3354/dao056163>
- Swaleh, M. M., Ruwa, R. K., Wainaina, M. N., Ojwang, L. M., Shikuku, S. L., & Maghanga, J. K. (2016). Heavy metals bioaccumulation in edible marine bivalve mollusks of Tudor Creek Mombasa Kenya. *IOSR Journal of Environmental Science, Toxicology and Food Technology*. <https://doi.org/10.9790/2402-1008024352>
- Taylor, C. L. (2008). Highlights of a model for establishing upper levels of intake for nutrients and related substances: Report of a joint FAO/WHO technical workshop on nutrient risk assessment, May 2-6, 2005.' *Nutrition Reviews*, *65*(1), 31–38. <https://doi.org/10.1111/j.1753-4887.2007.tb00265.x>
- The Department of Industrial Works. (2021). Industrial factories data in Kantang District, Trang province in August 2021 [Online]. Available <http://reg.diw.go.th/executive/Amp3.asp?amp=2&prov=92> (21 December 2020)

- United States Environmental Protection Agency (USEPA) (2002). A review of the reference dose and reference concentration process (EPA/630/P-02/002F). Washington DC: Risk assessment forum.
- USEPA IRIS (US Environmental Protection Agency)'s Integrated Risk Information System. (2011). "Environmental protection agency region I, Washington DC 20460." Retrieved August 14, 2021, from <http://www.epa.gov/iris/>.
- Vaezzadeh, V., Zakaria, M. P., Bong, C. W., Masood, N., Magam, S. M., & Alkhadher, S. a. A. (2017). Mangrove oyster (*Crassostrea belcheri*) as a biomonitor species for bioavailability of Polycyclic Aromatic Hydrocarbons (PAHs) from Sediment of the West Coast of Peninsular Malaysia. *Polycyclic Aromatic Compounds*, 39(5), 470–485. <https://doi.org/10.1080/10406638.2017.1348366>
- Wang, L., Wang, X., Chen, H., Wang, Z., & Jia, X. (2022). Oyster arsenic, cadmium, copper, mercury, lead and zinc levels in the northern South China Sea: long-term spatiotemporal distributions, combined effects, and risk assessment to human health. *Environmental Science and Pollution Research*, 29(9), 12706–12719. <https://doi.org/10.1007/s11356-021-18150-6>
- Wang, W., Meng, J., & Weng, N. (2018). Trace metals in oysters: molecular and cellular mechanisms and ecotoxicological impacts. *Environmental Science: Processes & Impacts*, 20(6), 892–912. <https://doi.org/10.1039/c8em00069g>
- Wanick, R. C., Kütter, V. T., Teixeira, C. L., Cordeiro, R. C., & Santelli, R. E. (2012). Use of the digestive gland of the oyster *Crassostrea rhizophorae* (Guilding, 1828) as a bioindicator of Zn, Cd and Cu contamination in estuarine sediments (south-east Brazil). *Chemistry and Ecology*, 28(2), 103–111. <https://doi.org/10.1080/02757540.2011.638630>
- WORMS - World Register of Marine Species. (2018). Retrieved from <https://www.marinespecies.org/aphia.php?p=taxdetails>
- Wuana, R. A., Ogbodo, C. G., Itodo, A. U., & Eneji, I. S. (2020). Ecological and human health risk assessment of toxic metals in water, sediment and fish from lower Usuma Dam, Abuja, Nigeria. *Journal of Geoscience and Environment Protection*, 08(05), 82–106.

- Xiuzhen, S., Wenbin, Z., & Sulian, R. (2003). Structure and function of the digestive system of *Solen Grandis* Dunker. *Journal of Ocean University of Qingdao*, 2(2), 155–159. <https://doi.org/10.1007/s11802-003-0044-x>
- Yang, S., Cheng, F., Wu, X., Xing, Y., Gu, Z., & Tang, X. (2020). Length-weight relationship and growth of a marine gastropod mollusk, *Hemifusus ternatanus* (Gmelin) (Family: Melongenidae). *Pakistan Journal of Zoology*, 52(6). <https://doi.org/10.17582/journal.pjz/20180820030834>
- Yavaşoğlu, A., Dilara, O., Güner, A., Katalay, S., Oltulu, F., & Yavaşoğlu, N. Ü. K. (2016). Histopathological and apoptotic changes on marine mussels *Mytilus galloprovincialis* (Lamarck, 1819) following exposure to environmental pollutants. *Marine Pollution Bulletin*, 109(1), 184–191. <https://doi.org/10.1016/j.marpolbul.2016.05.084>
- Yonge, C. M. (1926). Structure and physiology of the organs of feeding and digestion in *Ostrea edulis*. *Journal of the Marine Biological Association of the United Kingdom*, 14(2), 295–386. <https://doi.org/10.1017/s002531540000789x>
- Zhang, X., Ye, B., Gu, Z., Li, M., Yang, S., Wang, A., & Liu, C. (2021). Comparison in growth, feeding, and metabolism between a fast-growing selective strain and a cultured population of pearl oyster (*Pinctada fucata martensii*). *Frontiers in Marine Science*, 8. <https://doi.org/10.3389/fmars.2021.770702>
- Zhang, Y., Qin, Y., Ma, L., Zhou, Z., Xiao, S., Ma, H., & Yu, Z. (2019). Gametogenesis from the early history lifes stages of the Kumamoto oyster *Crassostrea sikamea* and their breeding potential evaluation. *Frontiers in Physiology*, 10. <https://doi.org/10.3389/fphys.2019.00524>

BIOGRAPHY

Name-Surname	Kitiya Kongthong
Date of Birth	27 April 1992
Address	Faculty of Medical Science, Naresuan University, Phisanulok, Thailand
Current Workplace	A Master's student in Medical Science, Faculty of Medical Science, Naresuan University.
Current Position	Naresuan university
Work Experience	<ol style="list-style-type: none">1. Hematological laboratory staff at Meungake Veterinary Hospital, Chonburi, Thailand.2. Research assistant at NKC Institute of Gastroenterology and Hepatology, Songklanakarind Hospital, Songkhla, Thailand.
Education Background	Bachelor's degree in Marine Science (Marine Biotechnology) Faculty of Science and Fisheries Technology. Rajamangala University of Technology Srivijaya Trang Campus, Thailand.
Publication	<ol style="list-style-type: none">1. Kongthong K., Charoenphon N., Thaochan N., Boonyoung P, Iida A., Jeamah A, Imsonpang S., Wongkhamhaeng K, Kongtueng P., and Senarat S. (2023). A histological method for marine invertebrates. <i>Veterinary Integrative Sciences</i>, 21(1): 251-263.2. Kongthong, K., Senarat, S., Inchan, A., Kaneko, G., Iida, A., Phoungpetchara, I., Charoenphon, N. (2023). Size distribution and organ development of the hooded oyster, <i>Saccostrea cucullata</i> (Born, 1778) from Libong Island, Thailand. <i>ScienceAsia</i>, 49(6): 918-926.3. Senarat, S., Sapon, A., Kettratad, J., Angsujinda, K., Charoenphon, N., Kosiyachinda, P., Kongthong, K., Poolprasert, P., Boonyoung, P., & Kongtueng, P. (2023). Erythrocytic Nuclear Abnormalities and Leucocyte Profiles of Asian Seabass (<i>Lates calcarifer</i>) Exposed to Polluted Seawater. <i>Sains Malaysiana</i>, 52(4): 1059–1068.
Awards	<ol style="list-style-type: none">1. The Popular Vote Award 2023 entitled “A modified histological method for marine invertebrates” in thesis & independent study innovation awards 2023. June 16th, Naresuan University, Phitsanulok, Thailand.2. The Bronze Award in an oral presentation entitled “Characterization and Density of Mucous Secreting Cells of the Hooded Oyster, <i>Saccostrea cucullata</i> (Born, 1778)

from Libong Island, Thailand” in the 2nd Academic Conference on Agricultural Innovation and Natural Resources 2023. August 3rd-4th, Faculty of Natural Resources, Songkhla, Thailand.

